Turun yliopisto
University of Turku

COMPUTED TOMOGRAPHY AND RADIOGRAPHY IN THE DIAGNOSIS AND FOLLOW-UP OF PERIPROSTHETIC OSTEOLYSIS AFTER TOTAL ANKLE ARTHROPLASTY

Ia Kohonen

University of Turku

Faculty of Medicine

Department of Radiology

University of Turku Doctoral Programme of Clinical Investigation

Medical Imaging Centre of Southwest Finland, Turku University Hospital

Supervised by

Adjunct professor Kimmo Mattila
Department of Radiology
University of Turku
Turku, Finland

Reviewed by

Adjunct professor Martina Lohman
Department of Radiology
University of Helsinki
Helsinki, Finland

Professor Juhana Leppilahti
Department of Surgery,
Division of Orthopaedic and Trauma Surgery
University of Oulu
Oulu, Finland

Opponent

Professor Jaakko Niinimäki
Department of Radiology
University of Oulu
Oulu, Finland

*To Perttu
and the rest of my family*

ABSTRACT

Ia Kohonen

COMPUTED TOMOGRAPHY AND RADIOGRAPHY IN THE DIAGNOSIS AND FOLLOW-UP OF PERIPROSTHETIC OSTEOLYSIS AFTER TOTAL ANKLE ARTHROPLASTY

University of Turku, Faculty of Medicine, Department of Radiology, University of Turku Doctoral Programme of Clinical Investigation, Medical Imaging Centre of Southwest Finland, Turku University Hospital

Periprosthetic osteolysis is one of the most significant long-term complications after total ankle arthroplasty (TAA). The exact pathogenesis of osteolysis is unclear. It is a biological process involving many factors, mechanical factors probably, as well. Osteolysis is a progressive phenomenon which may lead to component failure.

Traditionally, patients with an ankle prosthesis are monitored only by radiography. In this study the incidence of periprosthetic osteolysis around TAAs was evaluated by radiographs and computed tomography (CT). These two methods were also compared for detection of osteolytic lesions around the prosthesis components. Acquisition parameters and positioning were studied for optimal imaging of total ankle prostheses on CT. TAAs were monitored by CT after bone grafting of osteolytic lesions and also the patients' symptoms after bone grafting were evaluated.

Early-onset TAA-associated periprosthetic osteolysis was common after arthroplasty. CT showed more and larger periprosthetic osteolytic lesions than radiographs around TAAs, especially around the talar component. CT proved to be a reliable imaging modality for studying periprosthetic lesions adjacent to ankle prostheses. Image artifacts on CT caused by the metal prosthesis components were small when acquisition parameters and, especially, orientation of the prosthesis in relation to the x-ray tube were optimal. Radiologically, progression of osteolysis continued in spite of bone grafting of periprosthetic osteolytic lesions around TAAs.

We recommend adding ankle CT to the postoperative follow-up for patients with suspected or known periprosthetic osteolytic lesions on radiographs. CT is also useful when evaluating periprosthetic bone stock before a reoperation.

Keywords: computed tomography, metal artifact, total ankle arthroplasty, osteolysis

TIIVISTELMÄ

Ia Kohonen

NILKAN TEKONIVELEEN LIITTYVÄN OSTEOLYYSIN DIAGNOSTIIKKA JA SEURANTA TIETOKONETOMOGRAFIA- JA RTG-KUVAUKSELLA

Turun yliopisto, Lääketieteellinen tiedekunta, Diagnostinen radiologia, Turun yliopiston kliininen tohtoriohjelma, Varsinais-Suomen kuvantamiskeskus, Turun yliopistollinen keskussairaala

Tekonivelen ympärille ilmaantuva osteolyysi on merkittävimpiä nilkan tekonivelleikkauksen myöhäisvaiheen komplikaatioita. Osteolyysin patogeneesiä ei täysin tunneta. Se on monitekijäinen biologinen prosessi, johon myös mekaaniset tekijät vaikuttavat. Osteolyysi on etenevä prosessi, joka pahimmillaan johtaa tekonivelen irtoamiseen.

Potilaita, joilla on nilkan tekonivel, on perinteisesti kuvannettu ainoastaan natiiviröntgenkuvilla. Tässä tutkimuksessa nilkan tekonivelen ympärillä esiintyvää osteolyysiä tutkittiin röntgen- ja tietokonetomografiakuvauksella (TT); näitä kuvantamismenetelmiä myös verrattiin toisiinsa osteolyysimuutosten havaitsemisessa. Sen lisäksi etsittiin optimaalisia kuvausparametreja ja -asentoa ajatellen nilkan tekonivelen TT-kuvausta. Nilkan tekoniveliä seurattiin TT-kuvauksella osteolyysimuutosten luusiirretäytön jälkeen. Lisäksi potilaiden kliinisiä oireita tarkasteltiin näiden uusintaleikkausten jälkeen.

Nilkan tekonivelten ympärillä havaittiin runsaasti osteolyysiä jo varsin varhaisessa vaiheessa tekonivelleikkauksen jälkeen. TT-kuvaus havaitsi enemmän ja kookkaampia muutoksia kuin röntgenkuvaus. Erityisesti telaluussa olevien osteolyysimuutosten arvioinnissa TT-kuvaus osoittautui hyödylliseksi kuvantamismenetelmäksi. TT-kuvaus oli luotettava kuvattaessa tekonivelen ympärillä olevia osteolyysimuutoksia. Metalliosien aiheuttamat artefaktat TT-kuvissa jäivät vähäisiksi, kun kuvausparametrit ja erityisesti tekonivelen asento suhteessa kuvausputkeen olivat optimaaliset. Osteolyysimuutosten luusiirretäytön jälkeen osteolyysin radiologinen progressio oli tavallista.

Nilkan tekonivelen TT-kuvaus on suositeltavaa potilaille, joiden röntgenkuvissa on todettu tai epäilty osteolyysiä tekonivelen ympärillä. TT-kuvaus on myös hyödyllinen arvioitaessa luurakennetta tekonivelen ympärillä ennen uusintaleikkausta.

Avainsanat: tietokonetomografia, metalliartefakta, nilkan tekonivel, osteolyysi

TABLE OF CONTENTS

ABBREVIATIONS AND DEFINITIONS

ALARA	As low as reasonably achievable
ArCom	Argon packaged Compression molded
BEI-SEM	Backscattered electron imaging-scanning electron microscope
BMI	Body mass index
BMP-7	Bone morphogenetic protein-7
CNR	Contrast-to-noise ratio
CRPS	Complex regional pain syndrome
CT	Computed tomography
DECT	Dual-energy computed tomography
ECTS	Extended CT scale
ED	Effective dose
EDX	Energy dispersive radiographic analysis
FBP	Filtered back projection
FDA	Food and Drug Administration
HA	Hydroxyapatite
HU	Hounsfield unit
IL-1β, IL-6	Interleukin-1beta, Interleukin-6
ICP-MS	Inductively coupled plasma mass spectrometry
IR	Iterative reconstruction
MAR	Metal artifact reduction
MARS	Metal artifact reduction sequence
MMP	Matrix metalloproteinase
MRI	Magnetic resonance imaging
OPG	Osteoprotegerin
PGE2	Prostaglandin E2
RANK	Receptor activator of nuclear factor kappa-B
RANK-L	Receptor activator of nuclear factor kappa-B ligand

SD	Standard deviation
SECT	Single-energy computed tomography
TAA	Total ankle arthroplasty
THA	Total hip arthroplasty
Ti	Titanium
TNF-α	Tumor necrosis factor alpha
UHMWPE	Ultra-high molecular weight polyethylene

LIST OF ORIGINAL PUBLICATIONS

This thesis is based on the following original publications, which are referred to in the text by Roman numerals I-IV.

I   Koivu H, Kohonen I, Sipola E, Alanen K, Vahlberg T, Tiusanen H. Severe periprosthetic osteolytic lesions after the Ankle Evolutive System total ankle replacement. J Bone Joint Surg Br 2009;91:907-14.

II   Kohonen I, Koivu H, Pudas T, Tiusanen H, Vahlberg T, Mattila K. Does Computed Tomography Add Information on Radiographic Analysis in Detecting Periprosthetic Osteolysis After Total Ankle Arthroplasty. Foot Ankle Int 2013;34:180-8.

III Kohonen I, Koivu H, Vahlberg T, Larjava H, Mattila K. Total ankle arthroplasty: optimizing computed tomography imaging protocol. Skeletal Radiol 2013;42:1507-13.

IV   Kohonen I, Koivu H, Tiusanen H, Kankare J, Vahlberg T, Mattila K. Are periprosthetic osteolytic lesions in ankle worth bone grafting? Submitted for publication.

The original publications have been reprinted with the permission of the copyright holders.

1. INTRODUCTION

Primary osteoarthritis is less common in the ankle than the hip and knee, but post-traumatic arthritis is quite frequent in the ankle. Inflammatory arthritis can also destroy ankle joint. Ankle arthrodesis was for a long time the only surgical procedure available to treat end-stage arthritis of the ankle. Ankle arthroplasty has emerged as an alternative procedure for selected patients.

The first-generation total ankle arthroplasties in the 1970s and 1980s were non-anatomical and did not respect ankle kinematics. Survivorship of these prostheses was poor and they were abandoned several years ago (Valderrabano et al. 2012, Gougoulias and Maffulli 2013). Today, TAA implants are non-cemented and have a two- or three-component design with mobile or fixed bearing polyethylene. Modern ankle prostheses provide acceptable survivorship rates. However, long-term survivorship of TAAs is still inferior to hip and knee prostheses. One of the most common complications related to TAA is osteolysis (Besse et al. 2009, Koivu et al. 2009, Henricson et al. 2011).

Osteolysis is an unresolved enigma. It is a complex biological process with a multifactorial etiology to which mechanical factors probably contribute. It has been commonly regarded as a foreign body reaction related to polyethylene, cement or metallic wear particles which stimulate the RANK/RANK-L/OPG pathway (Purdue et al. 2007, Ollivere et al. 2012). Interestingly, in some TAAs with osteolysis the amount of wear debris has been low but tissue necrosis has been extensive (Koivu et al. 2012, Dalat et al. 2013). Findings like this have generated a new hypothesis according to which the RANK/RANK-L/OPG pathway might be activated by necrotic autogenous tissue rather than by wear particles (Koivu et al. 2015).

Patients with total ankle prosthesis are traditionally monitored by plain radiography. Radiographs, however, give limited information on the periprosthetic bone compared to CT. Osteolytic lesions beneath the talar component are especially difficult to detect on radiographs ([1]Kohonen et al. 2013). All metallic components cause artifacts on CT which impair image quality. Today, artifacts caused by metal in the scanning field can be handled more adequately than before on CT. This is done by a sufficiently high tube voltage (kVp) and tube current (mAs) which decreases noise in images. Artifacts are also diminished by reduced pitch settings and narrow collimation. The disadvantage of these methods is that they increase the radiation dose. The orientation of the ankle prosthesis during scanning also affects artifact generation. Artifacts are most intense in the direction of the greatest cross-sectional profile of the prosthesis. The geometry, size and material of the implant

affect the artifacts. Metal artifacts can also be diminished in the post-processing phase. Increasing thickness of the reformatted images and appropriate soft-tissue algorithms minimize metal artifacts (Lee et al. 2007, Kataoka et al. 2010). Due to the 3-dimensional nature of the artifacts reformats along certain planes may further help to minimize interference from the artifact over the region of interest (Kataoka et al. 2010). Iterative reconstruction, a novel metal artifact reduction (MAR) image reconstruction algorithm, can also be used (Morsbach et al. 2013, Willemink et al. 2013, Boudabbous et al. 2015). Dual-energy CT (DECT), a new technique for musculoskeletal imaging (Nicolau et al. 2012), uses two different kilovolt peaks during imaging. The resulted data is combined mathematically to yield virtual monochromatic images. Beam hardening artifacts can be diminished by the use of DECT (Bamberg et al. 2011, Filograna et al. 2015).

This study arose from our observation of an increasing number of osteolytic lesions around TAAs on radiographs. From before it is known that radiographs underestimate the size of osteolytic lesions around total hip arthroplasty compared to CT (Puri et al. 2002, Walde et al. 2005); the same might be true for TAAs. In this study we thus have evaluated whether CT adds to the information provided by radiographs for detecting osteolysis after TAA. We also studied the optimal acquisition parameters and orientation of the ankle arthroplasty for minimizing metal artifacts on CT. A medium-term CT-follow-up of bone-grafted periprosthetic osteolytic lesions of ankles was performed.

2. REVIEW OF THE LITERATURE

2.1. Total ankle arthroplasty

2.1.1. Ankle joint

The ankle joint consists of the tibiotalar joint (upper ankle joint) and the talocalcaneal joint (subtalar joint). They act together and form a fundamental structure in the locomotor system of the human body. The inferior tibiofibular and fibulotalar joints are also part of the ankle joint complex. The medial collateral ligament (deltoid) and the lateral collateral ligament (anterior talofibular, posterior talofibular and calcaneofibular) are located around the ankle joint. Between the distal tibia and fibula lies the fibrous syndesmotic complex. It is an important structure for maintaining the stability of the ankle joint and consists of the distal anterior tibiofibular ligament, distal posterior tibiofibular ligament and the interosseous membrane (Figure 1).
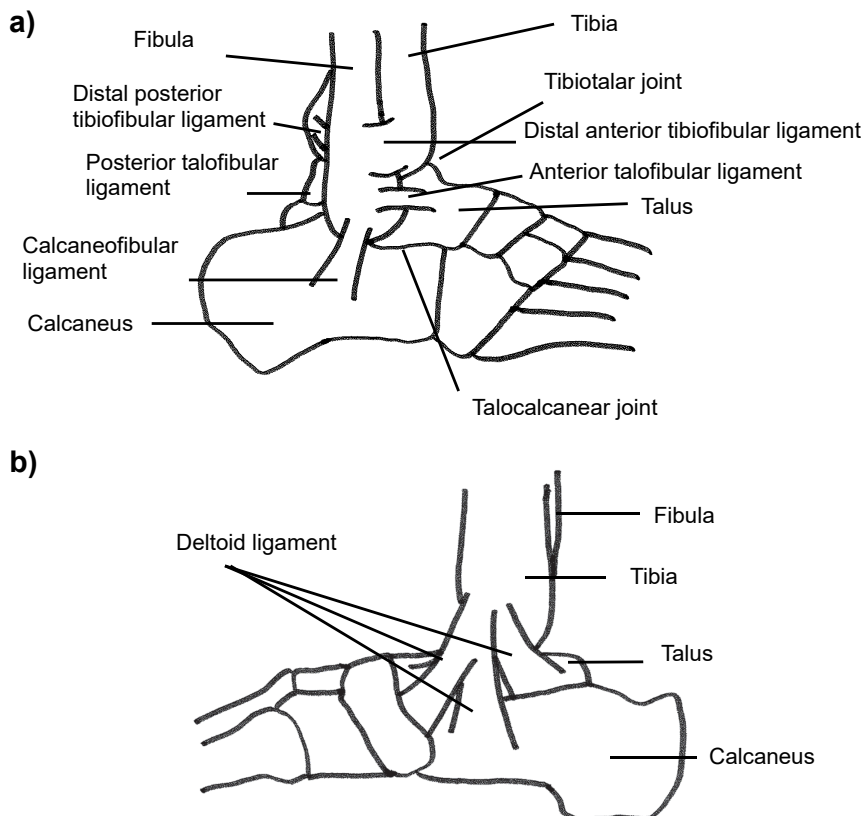

Figure 1. Anatomy of the ankle joint; lateral **a)** and medial **b)** view.

2.1.2. History of total ankle arthroplasty

Primary osteoarthritis of the ankle is less common than the hip or knee. However, post-traumatic arthritis in ankle occurs quite frequently. Also, patients with rheumatoid arthritis may develop severe ankle deformation. For many decades, ankle arthrodesis was the only surgical procedure available to treat end-stage arthritis of ankle, and it is still considered as the 'gold standard'. However, ankle arthroplasty has emerged as an alternative procedure to arthrodesis in selected patients to treat severe ankle changes.

The first total ankle arthroplasty was performed in 1970, described as a 'reverse hip arthroplasty procedure' (Lord and Marotte 1980). A metallic component with a long stem was placed in distal tibia. It articulated with a cemented acetabular cup in the calcaneus or talus. In the first operations the talus was completely removed. Altogether 25 total ankle arthroplasties were done, either tibio-calcaneal or tibio-talar. Only 7 were considered to be satisfactory. After these 25 operations the method was rejected and arthrodesis was recommended as the treatment of choice for severe upper ankle joint destruction (Lord and Marotte 1980).

Most first-generation TAA designs were 2-component models, and the prosthesis components were placed in the distal tibia and talus. Cement fixation was widely used in hip and knee replacements at that time, and thus cement was a logical choice also for ankle prosthesis fixation. Howmedica (Howmedica, Rutherford, NJ, USA) and Smith (Dow Corning, Arlington, TN, USA) are examples of these prostheses models (Valderrabano et al. 2012). The first-generation TAA designs were associated with high complication rates: osteolysis, loosening, subsidence and mechanical failure were the main reasons for failure. Cement fixation needed larger bone resections and this made revision surgery highly demanding. Clearly, further development of prosthesis models was essential.

In the second half of the 1980s, the TAA components underwent significant modifications. Cement was abandoned, which resulted in more limited bone resections. Later, 3-component fixed and mobile-bearing implants were introduced (Valderrabano et al. 2012). The 3-component prostheses consist of metallic tibial and talar components and a polyethylene (ultrahigh molecular weight polyethylene, UHMWPE) meniscus. The meniscus between the tibial and talar metal components may either be fixed with one of the components or remain mobile between them. Agility (DePuy, Warsaw, IN, USA), Inbone Total Ankle System (Wright Medical technology, Arlington, TX, USA) and ESKA (ESKA, Lubeck, Germany) are examples of 3-component, fixed bearing prostheses. These prostheses, although consisting of three pieces (tibial, talar and polyethylene), act as a two-component design. BP prosthesis (Endotec, Orange, NJ, USA), Ankle Evolutive System (Biomet, Warsaw,

Indiana, USA), STAR (Waldemar Link, Hamburg, Germany) and Hintegra (Newdeal SA, Lyon, France) are true 3-component, mobile-bearing prostheses. In Europe the most common implanted ankle prostheses are 3-component designs. In these prostheses a hydroxyapatite coating is often used to improve component fixation to the bone. In the United States FDA gave approval to the first 3-component prosthesis as late as 2009. The prosthesis model was STAR (Scandinavian Total Ankle Replacement). Recently, the trend is towards 3-component mobile-bearing implants also in the United States.

2.1.3. Survivorship of total ankle arthroplasty

Survivorship of first-generation TAAs was poor (Lord and Marotte 1980, Bolton-Maggs et al. 1985*).* In the beginning, large bone resections resulted in weakened bone in the distal tibia and talus. Sparing bone cuts with modern implants have been less vulnerable to the drawbacks of resected bones. The survivorship rates of modern ankle prosthesis models are acceptable, but the long-term survivorship of total ankle arthroplasty is shorter than of hip and knee arthroplasties. Total ankle arthroplasty is technically demanding for the ankle surgeon, and the learning curve is flat (Henricson et al. 2007).

The biomechanics of the ankle joint is exquisitely complex – the ankle is certainly not only a hinge joint. It allows movement in three planes in the tibiotalar and talocalcaneal joints: plantar flexion and dorsiflexion, external and internal rotation and inversion and eversion. Large forces are absorbed over a small area when the patient is standing (Vickerstaff et al. 2007, Park and Mroczek 2011). A thorough understanding of ankle joint anatomy and function is crucial when trying to design the most optimal prosthesis model for ankle joint.

One of the crucial steps in the TAA procedure is correct positioning of the prosthesis components, especially the talar component. Intraoperative complications of TAA include malposition of the talar component (Valderrabano et al. 2012), injuries to neurovascular and tendinous structures, improper sizing of prosthesis components, inadequate bone resections and malleolar fractures. Postoperatively, recovery may be impaired due to infection, poor wound healing, edema and stress fractures in the early postoperative phase. Later osteolysis, aseptic loosening, deep infections, periprosthetic fractures, component wear, heterotopic ossification and complex regional pain syndrome (CRPS) may ensue (Bestic et al. 2008, Hsu et al. 2015). Many studies have reported that osteolysis and aseptic loosening are the most common complications related to total ankle prosthesis (Knecht et al. 2004, Koivu et al. 2009, Gupta et al. 2010, Krause et al. 2011, Nieuwe Weme et al. 2015, Mercer et al. 2016*).*

Optimal preoperative patient selection is important to minimize the risk of complications. Absolute contraindications for total ankle arthroplasty are infection, Charcot's arthropathy, avascular necrosis of the talus, inadequate foot musculature, paralysis and severe joint malalignment. Relative contraindications include diabetes, smoking, high body mass index, heavy physical work and young age (Gougoulias et al. 2009).

The 5-year survivorship rates of TAA vary from 70% to 93% (Anderson et al. 2003, Wood and Deakin 2003, Knecht et al. 2004, Haddad et al. 2007, Henricson et al. 2007, Skyttä et al. 2010) and the 8- to 10-year survivorship from 69% to 90% (Doets et al. 2006, Haddad et al. 2007, Henricson et al. 2011, Mann et al. 2011, Zaidi et al. 2013). A review article citing 13 articles summarizes that the survivorship of TAA-prostheses ranges from 67% at 6 years to 95% at 12 years (Gougoulias et al. 2010). There are studies showing that the survivorship of TAA is lower in younger patients (Haddad et al. 2007, Henricson et al. 2007). Some studies have reported poorer outcome in patients who have undergone TAA because of post-traumatic arthritis than osteoarthritis and rheumatoid arthritis. The reason for this may be a younger patient age in the post-traumatic TAA group. Additionally, most of these patients have had previous surgery of the ankle (Valderrabano et al. 2004, Henricson et al. 2007) and this, in itself, may impair TAA survivorship. On the other hand, there are studies that have not found an association between TAA survivorship and patient age (Kofoed and Lundberg-Jensen 1999, Demetracopoulos et al. 2015).

Valderrabano et al. studied sporting activity after TAA and they reported excellent or good outcomes in 83% of cases (Valderrabano et al. 2006). The mean range of motion rose from 21° to 35°. Also, the sports activity level rose. However, the patients active in sports before the operation were the active ones also after TAA. The most popular sporting activities after TAA were hiking, biking and swimming. Patient satisfaction and postoperative pain was studied in a review article (Gougoulias et al. 2010). Residual pain after TAA was common; it was reported by 23-60% of the subjects. Patient satisfaction was high, 79-97%, despite a high amount of residual pain. However, rigorously validated scales to evaluate patient satisfaction were not used, which raises concern of methodologic flaws (Gougoulias et al. 2010).

Ankle arthrodesis is still considered to be the surgical 'gold standard' in most studies. The total number of ankle arthroplasties is increasing and competes favorably with ankle arthrodesis. According to a meta-analysis, the intermediate-term outcome for TAA and arthrodesis is similar (Haddad et al. 2007), as has been reported in subsequent separate studies (Krause et al. 2011, Daniels et al. 2014). Gait and range of motion remain better after TAA (Easley et al. 2011) and arthritis of the neighboring joints is potentially less prominent after TAA than after ankle

arthrodesis (Coester et al. 2001, Easley et al. 2011, Mann et al. 2011). According to some studies the rate of reoperations is higher after TAA (Krause et al. 2011, Daniels et al. 2014) than after arthrodesis.

2.2. Periprosthetic osteolysis

2.2.1. Pathogenesis of periprosthetic osteolysis

Periprosthetic osteolysis is a common complication which threatens the long-term survivorship of total joint replacements. The exact pathogenesis of osteolysis is still not fully understood (Purdue et al. 2007, Koivu et al. 2009, Ollivere et al. 2012, van Wijngaarden et al. 2015). Osteolysis is a biological process with a multifactorial etiology, including mechanical factors. Several different cell types are involved in this complex biological cascade.

Osteolysis was originally described as 'cement disease'. It was thought that the cement used originally with many total joint arthroplasty designs was the cause for osteolytic lesions. Harris et al. (1976) and Willert and Semlitsch (1977) were the first to publish the biological response to wear debris and how it relates to periprosthetic osteolysis. It is commonly considered that a foreign body reaction due not only to cement but also to polyethylene and metallic wear particles is an important contributor to the process of osteolysis (Cottrino et al. 2016). Hydroxyapatite coating of the implant may also play a role in TAA osteolysis (Singh et al. 2016). Macrophages are probably the most important cellular targets of wear debris (Purdue et al. 2007). Wear particles are phagocytosed by macrophages, which results in induction of proinflammatory mediators, such as tumor necrosis factor alpha (TNF-α), prostaglandin E2 (PGE2), interleukin-1beta (IL-1β) and interleukin-6 (IL-6) (Ollivere et al. 2012). Wear particles are considered to be one of the leading culprits of periprosthetic osteolytic lesions. The specific nature of the foreign body response depends on many parameters, e.g., size, shape, composition, volume and surface area of the wear particles (Purdue et al. 2007).

The RANK/RANK-L/OPG pathway plays a central role in osteoclastogenesis and osteolysis (Ollivere et al. 2012). Osteoclasts break down bone tissue and the RANK receptor is a membrane receptor found primarily on osteoclasts. Ligand (RANK-L) binding to the receptor induces osteoclast formation and activity. Osteoprotegerin (OPG) antagonizes this cascade. RANK-L expression is increased in osteolytic cavities around prosthesis components, specifically in macrophages, giant cells and fibroblasts (Holding et al. 2006, Ollivere et al. 2012). TNF-α and other proinflammatory mediators enhance osteoclast formation directly or indirectly by stimulating RANK-L/RANK osteoclast formation in areas of aggressive

periprosthetic osteolysis (Holding et al. 2006). Expression and secretion of matrix metalloproteinases (MMPs) by macrophages are also enhanced in the tissues around periprosthetic osteolysis. MMPs are well-known extracellular matrix degrading enzymes (Archibeck et al. 2001).

Interestingly, in some TAAs the amount of wear debris has been low despite massive osteolysis (Koivu et al. 2009, Koivu et al. 2012, Dalat et al. 2013) and, also polyethylene inlays have appeared intact at surgery (Koivu et al. 2009). Some recent studies have reported extensive tissue necrosis in failed TAAs (Koivu et al. 2012, Dalat et al. 2013). Such findings have generated a new hypothesis according to which the RANK/RANK-L/OPG pathway is activated by necrotic autogenous tissue rather than by wear particles in patients with osteolysis-associated TAAs (Koivu et al. 2015). There are several theories to explain necrotic tissue formation, e.g., local damage during operation, early walking after operation, and high fluid pressure in the joint cavity. None of these theories has yet been proven correct and intense research is going on.

Under normal conditions, there is a balance between bone formation and resorption which allows for homeostasis and bone remodeling. Osteoblasts are responsible for bone formation and osteoclasts for bone resorption. Much effort has been put on explaining massive bone resorption related to periprosthetic osteolysis. Importantly, wear particles may also impact on bone formation by inhibiting it, since wear particles reduce the expression of collagen types I and III by osteoblasts (Vermes et al. 2000, Purdue et al. 2006).

2.2.2. Osteolysis around total joint arthroplasty

Periprosthetic osteolysis is the leading complication after an otherwise successful surgical procedure, total joint arthroplasty. Osteolysis related to total hip arthroplasty has been studied for many years. Osteolysis occurs also in connection with other total joint arthroplasties. Total hip arthroplasty studies have shown that the mean time from surgery to radiographically detectable osteolytic lesions varies from five to ten years (Puri et al. 2002, Park et al. 2004). Looney et al. reported an association between acetabular osteolysis and polyethylene wear (Looney et al. 2002). In another study such an association was not found, which indicates that also other factors than polyethylene component wear affect the development of osteolytic lesions (Puri et al. 2002).

Osteolysis has been reported with numerous total ankle implant designs (Knecht et al. 2004, Valderrabano et al. 2004, Hanna et al. 2007, Gougoulias et al. 2010, Skyttä et al. 2010, Henricson et al. 2011, Daniels et al. 2014). In general, osteolysis around TAA appears sooner than around THA (Anderson et al. 2003, Haddad et al. 2007,

Henricson et al. 2011, Kokkonen et al. 2011), even very early after TAA with the Ankle Evolutive System (Biomet, Warsaw, Indiana, USA*)* (Besse et al. 2009, Koivu et al. 2009, Rodriguez et al. 2009, Kokkonen et al. 2011).

Patients may remain asymptomatic for a long time despite large osteolytic lesions around prosthesis components (Rodriguez et al. 2010). Because the osteolytic process is typically progressive (Purdue et al. 2007) and can finally lead in component failure, it is important to detect, localize, measure, and follow this phenomenon ([1]Kohonen et al. 2013). It is still unclear why periprosthetic osteolysis in some patients starts soon after TAA while some get it several years after the operation and others never face it.

2.2.3. Diagnostic imaging of osteolysis

Traditionally, patients with total joint prostheses are followed only by radiographs. Radiographically, osteolysis has been defined as a new or expanding lucency with sharply demarcated lines adjacent to prosthesis components (Puri et al. 2002). Many previous studies on THA have shown that radiographs underestimate the size of periprosthetic osteolytic lesions (Hozack et al. 1996, Puri et al. 2002). Indeed, some of the lesions may remain undetected and can only be seen on computed tomography (Looney et al. 2002). Studies on TAA-related osteolysis have shown similar findings: more and bigger osteolytic lesions have been found on CT compared to radiographs (Hanna et al. 2007, Koivu et al. 2009, Kokkonen et al. 2011, [1]Kohonen et al. 2013). The osteolytic lesions beneath the talar component are especially difficult to detect on radiographs ([1]Kohonen et al. 2013). Osteolytic lesions on CT appear as discrete, well-demarcated areas of lucency with no osseous trabeculae in the periprosthetic bone (Puri et al. 2002). Every metal object causes artifacts on CT and must be taken into consideration when metallic prostheses are examined. However, these artifacts are handled quite well in modern scanners which use modified acquisition parameters, newer imaging methods, and metal artifact reduction (MAR) image reconstruction algorithms.

CT is recommended for the follow-up of osteolytic lesions around TAAs. CT is mandatory when planning revision operations. In addition to depicting osteolytic lesions around prosthesis components, CT demonstrates remaining bone stock reliably (DiDomenico and Cross 2012).

MRI can also be used to evaluate periprosthetic osteolytic lesions. Metal implants cause artifacts also on MRI and impair the quality of the images. Metal artifact reduction sequences (MARS) are an effective way to improve the detection of lesions around the prosthesis components (Potter et al. 2005, Potter and Foo 2006, Vessely et al. 2006). However, in general practice CT is more often utilized

for evaluating periprosthetic osteolytic lesions than MRI due to better availability, faster imaging, and less cost. According to a study of Walde et al., the detection rate for smaller periacetabular osteolytic lesions in cadaver models was better on MRI than CT (Walde et al. 2005). Both of these imaging modalities were superior when compared to radiographs. To my knowledge similar data using TAA has not been published.

Digital tomosynthesis can also be a promising alternative for imaging joints with prostheses. It fuses cone beam CT reconstruction with digital imaging processing to produce images from a single tomography. Presently, there is not much scientific evidence of its superiority to other imaging modalities. Many published studies of tomosynthesis have been performed with total hip prostheses. (Göthlin and Geijer 2013, Tang et al. 2016).

2.2.4.   Treatment of TAA osteolysis

2.2.4.1. Surgical treatment

There is no standard surgical treatment protocol for osteolysis around TAAs. The general goal is to restore bone stock. Other principles are to remove the source of wear debris, debris itself, and necrotic tissue, if apparent (Stulberg and Della Valle 2008, Dalat et al. 2013, Koivu et al. 2015). Filling the osteolytic cysts is usually recommended, as is exchanging the polyethylene, although the exact role of polyethylene in the pathogenesis of osteolysis is unclear. A bone graft is often used to fill the osteolytic lesions around the TAA (Whittaker et al. 2008, Gupta et al. 2010, Gaden and Ollivere 2013, Yoon et al. 2014, Williams et al. 2015). Cement has occasionally been used as filling material of large osteolytic lesions (Kotnis et al. 2006), also with metal (Schuberth et al. 2011). The tibial and talar metallic components may remain intact if they are well fixed to bone at operation. If metallic components need to be exchanged, a longer stem prosthesis or custom-designed prosthesis components may be appropriate alternatives (Myerson and Won 2008, Whittaker et al. 2008, Gupta et al. 2010, Jonck and Myerson 2012, Ellington et al. 2013).

The decision when to operate patients with osteolytic lesions around TAA is made on an individual basis. A lesion that progresses during follow-up should be grafted (Mann et al. 2011). Grafting should be considered also if there are osteolytic lesions in multiple areas (Mann et al. 2011). Severe symptoms may also indicate operative treatment. However, it should be noted that a patient even with large osteolytic lesions around the TAA may be asymptomatic and the joint may function normally or be only slightly impaired. Osteolytic lesions beneath the talar component should be treated more aggressively than tibial lesions, because maintaining the bone stock

of the talus is difficult in the presence of large periprosthetic osteolytic lesions. Talar component subsidence can be very challenging to treat, and in some cases arthrodesis or even amputation may be the only alternative. According to a study on THA (Lavernia 1998), early intervention of structurally critical periprosthetic lytic lesions in fairly asymptomatic patients may be very cost-effective.

2.2.4.2. Nonsurgical treatment

There is no effective medical treatment for periprosthetic osteolysis around TAAs. There are some potentially useful candidate drugs for the treatment of periprosthetic osteolysis, mainly based on their performance in other indications. The bisphosphonates inhibit mature osteoclasts and teriparatide promotes osteoblast activity. Both of these drugs are approved for the treatment of osteoporosis. Anti-inflammatory agents traditionally used in rheumatoid arthritis, such as the COX-2-inhibitors and TNF-antagonists are other possible alternatives for the medical treatment of periprosthetic osteolysis. Denosumab is a promising drug, as well. It is a selective RANK-L antagonist and it has been approved for the treatment of osteoporosis. So far, there is very little clinical evidence on the effectiveness of these drugs in the treatment of osteolysis (Purdue et al. 2006, Schwarz 2008).

There is at least one case report in the literature of percutaneous treatment of periprosthetic osteolytic lesions in the knee of an elderly man. The osteolytic lesions were treated percutaneously by debridement and grafting, using an injectable calcium phosphate bone cement under fluoroscopic guidance (Atkinson et al. 2010). Percutaneous treatment could be a possible option also around total ankle arthroplasty of a patient having contraindication to surgery.

2.3. Computed tomography

2.3.1. History and evolution of CT

In the beginning of the 19th century, the Austrian mathematician Johann Radon found that the distribution of a material in an object layer can be calculated if the integral values along any number of lines travelling through the same layer are known (Kalender 2006). After that, several scientists attempted to apply this theorem to medical applications of reconstructive tomography (Kalender 2006). However, it took until 1972 when computed tomography was used for first time in clinical practice. This took place at the Atkinson Morley Hospital in London when a frontal lobe cystic tumor of the brain of a patient was examined by the British engineer, Godfrey Hounsfield (Hounsfield 1973). He has been recognized as the inventor of computed tomography.

The first commercial CT scanners, or second generation scanners, contained detector rows and small fan beams instead of pencil beams. Scan times were about 5 min per image, and image reconstruction took the same time. In the third-generation CT scanners, both the x-ray tube and the detector rotated around the patient, allowing whole body scanning instead of the brain only. At the end of 1970s, in the fourth-generation CT scanners, only the x-ray tube rotated, while the detector ring was stationary (Kalender 2006). With that improvement scan times were shortened to about 5 seconds per image. In the 1980s MRI developed rapidly and it was a common opinion that CT would soon be completely replaced by MRI. The abbreviation 'NMR', nuclear magnetic resonance, was even interpreted as 'No More Röntgen'. However, in the 1980s the scanning time of single CT slices declined and at the end of that decade spiral CT was introduced. Since the 1990s, the development of CT has been enormous. In the early 1990s, slice to slice imaging was replaced with spiral volumetric scanning also for clinical examinations. Scanning times were shortened and isotropic data became available. A few years later multirow detectors made multislice scanning possible (Kalender 2006). At the end of the 1990s scan times under 1 s per image were routinely available. In the first decade of the 2000s, more rows were added to the detector arrays. Very high image quality and isotropic data could be achieved even at very short examination times. Since then, PET/CT scanner, cone beam CT, dual-energy CT, and CT imaging on C-arm units have been introduced. Very fast scanning times have made cardiac CT, CT angiography, CT colonography, and CT guided interventional procedures possible. In the recent years research has focused on developing more sensitive detectors and postprocessing techniques, such as iterative reconstruction.

2.3.1.1. General principles of CT

The X-ray source and the detectors lie inside the gantry, opposite to each other. Usually the table is moving at constant speed during spiral volumetric scanning. The X-ray beam passes through the imaged area and a part of the radiation passes through a target to the detectors. A pixel (picture element) is the smallest unit of a computed tomogram. Depending on the size of scanned area and the image matrix, the pixel stands for a certain proportion of the total cross-sectional area. The area of the pixel and the slice thickness determine a volume element, the voxel. Each voxel is given a numerical value (attenuation value), which corresponds to the average amount of radiation absorbed by the tissue in that picture element. Attenuation values, measured in Hounsfield units (HU), are registered in the computer. Finally, a CT image is reconstructed. The translation of these numbers into analogous grey levels creates the images we are used to see.

2.3.2. Radiation dose

2.3.2.1. General aspects

CT subjects patients to the greatest amount of radiation of all imaging modalities. CT accounts for about 7% of all radiologic procedures in the world, but generates more than 40% of the average collective effective dose, in the United States almost 50% (Mettler et al. 2009). When scanning patients by CT, principles of justification and optimization should be followed. According to the justification principle, the benefits of the examination should be greater than the disadvantages. The ALARA (As Low As Reasonably Achievable) principle is used for guidance of optimization. The examination should be performed so that the radiation dose is lowest possible (Dougeni et al. 2012). Special attention should be paid to individuals whose disorder requires several controls by CT and also to pregnant women and children. The developing organs of children are more sensitive to radiation than the fully mature organs of adults. In addition, the longer life expectancy of children and possible repeated examinations later in life cause a greater risk of potential radiation damage to pediatric patients than adults (Dougeni et al. 2012).

2.3.2.2. Radiation dose measures

The question of radiation dose is unique to CT, since exposure is essentially continuous around the patient. The radiation dose is much larger at the entrance than the exit skin area, but the patient is exposed to radially symmetric radiation in CT scans with a full 360° rotation and this results in a symmetric dose gradient within the patient. In a uniform circular radiation dose phantom, all points at a certain radius from the center are subject to practically the same radiation dose. The absolute values of the absorbed doses are dependent on the object size. The longer the distance between the center and periphery is, the smaller are the radiation doses in the central areas of the object.

There are also dose variations along the length of the patient, i.e. the z-axis. The radiation is not limited to the primary area being imaged, since there are tails to this distribution from photon scatter and nonideal collimation of the x-ray source. If such tails are significant, these contributions add up and result in an additional absorbed dose in the primary area. The total radiation dose in a specific section consists of the sum of contributions to the section. There are several measures which account for the effects of multiple scans. The Computed Tomography Dose Index (CTDI) is defined as the radiation dose, normalized to beam width, measured from 14 contiguous sections (McNitt-Gray 2002). However, according to this definition only 14 sections could be measured and the radiation profile measurements (usually done by thermoluminescent dosimeters or film) are not

very useful. Another radiation dose index, $CTDI_{100}$, was developed to overcome the limitations of the CTDI. This index allows calculation for 100 mm along the length of an entire pencil ionization chamber. Further, $CTDI_{vol}$ takes into account the parameters that are related to a specific imaging protocol, the helical pitch or axial spacing. The $CTDI_{vol}$ is a standardized measure of the radiation output of a CT system (McCollough et al. 2011). The dose descriptor usually reported on CT consoles and related to $CTDI_{vol}$ is the dose-length product (DLP). The DLP is the $CTDI_{vol}$ multiplied by the length of the scan (McNitt-Gray 2002). This descriptor is used as an assessment of the Effective Dose (ED). The ED takes into consideration where the radiation dose is being absorbed. The absorbed radiation dose to every anatomic structure must be quantified. These values are then modified by specific tissue-weighting factors. The ED is a weighted average of organ doses adjusted to specific target tissues by the application of tissue-weighting factors (McNitt-Gray 2002, Biswas et al. 2009). It must be noted, however, that the ED is an average, since the measurements have been done with standard-sized phantoms for ethical reasons. Use of phantoms leads to underestimation of the actual absorbed dose for pediatric patients and, on the other hand, to overestimation of the actual absorbed dose for obese patients.

2.3.2.3. Factors that influence radiation dose

The energy of the x-ray beam (kVp) affects the radiation dose: increasing tube voltage increases the radiation dose. The photon fluence (mAs) affects also directly the radiation dose, and high mAs values increase radiation dose due to a higher number of detected photons. Automatic tube current modulation is clinical routine in modern scanners, i.e., the tube current is automatically adjusted to the size and geometry of the body part being scanned. This provides constant image quality, but the radiation dose decreases. The pitch (table translation in millimeters per gantry rotation/beam collimation) also affects the patient's radiation dose. Lowering the pitch settings increases the radiation dose, as does narrowing beam collimation (McNitt-Gray 2002). The scan length must also be taken into account. Scanning should include the minimum body length needed to make an accurate diagnosis (Costello et al. 2013). Dual-energy CT (DECT) can also decrease radiation dose when scanning metallic implants, since even low-dose DECT enables a reduction of artifacts due to metallic implants in a similar way as neutral-dose DECT and even more than reduced or neutral-dose single-energy computed tomography, SECT (Filograna et al. 2016).

In the post-processing phase, iterative reconstruction (IR) has the potential to improve image quality compared to traditionally used filtered back projection (FBP). Because of less image noise after iterative reconstruction compared to FBP

at the same radiation dose level, lower radiation doses can be used. However, low-contrast detectability probably cannot be preserved by low-dose CT protocols with iterative reconstruction algorithms. In one study the detectability of low-contrast phantom lesions was no better in association with IR compared to FBP (Schindera et al. 2013).

Patient size affects also the radiation dose. The effective dose is bigger for small patients compared to obese patients at the same dose level.

2.3.3. Metal artifacts

2.3.3.1. Type of metal artifacts
Metal objects cause artifacts on CT by distorting the image. There are several types of artifacts that metal object can cause. A metal object in the scanning field causes streaking artifacts because the density of the metal object is outside the normal range that can be handled by the computer. This results in incomplete attenuation profiles (Barret and Keat 2004). Insufficient photons reach the detectors and low photon counts cause noise in images, also called photon starvation.

Beam hardening artifacts are the result of the x-ray beam passing through a metal component. Lower energy photons are absorbed faster than higher energy photons. The beam becomes 'harder', and its mean energy increases. This phenomenon can cause either cupping artifacts or the appearance of dark bands or streaks between dense objects in the image. When x-rays pass through the middle portion of a uniform, cylindered phantom with more material they are hardened more than those passing through the edges. When the beam becomes harder, the attenuation rate decreases. When the beam reaches the detectors it is more intense than expected without the beam hardening effect. The final attenuation profile is not the same as the ideal and cupping artifacts are generated. Dark band or streak artifacts are formed in very heterogeneous cross sectional areas. When two dense objects are in the same area, the beam that passes through one object at a certain tube position is hardened less than when it passes through both objects at another tube position (Barret and Keat 2004).

Partial volume artifacts are generated when a dense metal object penetrates partway into the width of the x-ray beam. During scanning some detectors 'see' the object and others do not. The discrepancies between the views cause shading artifacts (Barret and Keat 2004).

The number of projections used to reconstruct a CT image affects the image quality. If there is a too wide interval between projections (undersampling),

computer information misregistration may result in areas of sharp edges or small objects. This leads to stripes in the image, called aliasing (Barret and Keat 2004).

2.3.3.2. Methods for decreasing metal artifacts

The methods used to decrease metal artifacts usually involve increased radiation dose. Increasing the tube voltage (kVp) increases the likelihood that the x-ray beam will penetrate metal and, theoretically, this can reduce metal artifacts. A higher kilovoltage reduces noise but diminishes image contrast. If the tube current (mAs) is increased, more photons reach the detector, and noise and artifacts are reduced. Both of these methods increase the radiation dose to the patient (Kataoka et al. 2010). When lowering the pitch settings, artifacts are diminished, but the radiation dose increases (Lee et al. 2007). Metal artifacts may be reduced with the use of a narrow collimation setting. Actually, thin-section acquisition is expected to reduce partial volume artifacts (Barret and Keat 2004). An Extended CT Scale (ECTS) technique can be used when imaging metal implants. In ECTS, it is possible to expand the Hounsfield scale from a standard maximum window of 4000 HU to 40 000 HU. The ECTS technique is based on the fact that the linear attenuation coefficients of metals are so high that they are outside the normal range of reconstructed CT numbers (Lee et al. 2007).

Orientation of the hardware during scanning affects artifact generation ([2]Kohonen et al. 2013). Artifacts are most pronounced in the direction of the hardware's greatest cross-sectional profile (Lee et al. 2007). To minimize these artifacts, the body part with the metal component inside should be aligned so that the x-ray beam traverses the smallest possible cross-sectional area of the metal component (Kataoka et al. 2010). The geometry, size, and composition of the implant also affect artifacts, but these circumstances cannot be changed. A large metal object causes more artifacts than a small and thin one. Titanium causes fewer artifacts than stainless steel or cobalt-chromium (Lee et al. 2007).

Metal artifacts can also be decreased in the post-processing phase. Increased slice thickness of the reformatted sections reduces metal-related artifacts (Lee et al. 2007). It is also important to choose the right reconstruction algorithm (kernel). Appropriate soft-tissue algorithms can minimize metal artifacts (Kataoka et al. 2010). Because artifacts between the x-ray beam and the hardware are 3-dimensional, reformats along certain planes may help minimizing interference from the artifact in the region of interest (Kataoka et al. 2010).

There are also newer metal artifact reduction (MAR) image reconstruction algorithms available: iterative reconstruction, projection interpolation, and

adaptive filtering methods. At first, there was uncertainty as to the benefits of these reconstruction softwares in reducing metal artifacts, the long computational time being one of the main limitations (Wang et al. 2008, Dougeni et al. 2012). Other limitations were induction of totally new artifacts, loss of detail in images, and lower image contrast near metallic implants (Watzke and Kalender 2004, Liu et al. 2009, Malan et al. 2012). However, there are increasing number of studies addressing the usefulness of these newer MAR image reconstruction algorithms and because of increased computational power their use has become more common in clinical practice (Morsbach et al. 2013, Willemink et al. 2013, Boudabbous et al. 2015).

Dual-energy CT (DECT) is a recent technique for musculoskeletal imaging to reduce artifacts caused by metallic implants (Bamberg et al. 2011, Nicolaou et al. 2012, Filograna et al. 2016, Sandgren et al. 2016). The basic principle of DECT is that two datasets with different kilovolt peaks are obtained from the same area. Low-energy and high-energy image data are combined mathematically resulting in virtual monochromatic images. The resulting images are less susceptible to beam hardening artifacts (Coupal et al. 2014).

3. AIMS OF THE PRESENT STUDY

The general aim of this study was to evaluate the role of CT and radiography for the diagnostic evaluation and follow-up of osteolysis around the prostheses of patients who have undergone total ankle arthroplasty (TAA).

The specific aims were:

1. To evaluate radiographically the incidence of periprosthetic osteolysis in Ankle Evolutive System (AES) TAAs and to define the possible risk factors for it. Also, to make microbiological and histological analysis of the samples around TAAs.

2. To compare the number and size of osteolytic lesions around TAAs recorded by radiography with those recorded by CT.

3. To evaluate the optimal parameters and positioning for CT-imaging of total ankle prosthesis.

4. To monitor osteolytic lesions around TAAs with CT after bone grafting and to study the association between the extent of osteolysis and the patient's symptoms.

4. SUBJECTS AND METHODS

4.1. Study design

The study consists of four sub-studies (I-IV). The arthroplasty operations and reoperations in this study were performed in the Turku University Hospital between 2000 and 2010.

The aim of the first sub-study was to evaluate periprosthetic osteolysis around total ankle arthroplasties on radiographs (Study I). In Study I also the histological and microbiological analysis of samples taken of the osteolytic lesions and adjacent structures was determined. In Study II the ability of radiographs and CT to depict and describe osteolytic lesions around TAA was compared. Study III evaluated the optimal parameters and positioning for imaging of total ankle prosthesis on CT. In the last sub-study (Study IV) CT was used to follow osteolytic lesions around TAA after bone grafting. Patients' symptoms and the function of their ankle joint were also determined.

4.2. Patients (Studies I, II, IV)

The number of the patients and prosthesis models by study are shown in Table 1.

Table 1. Patient populations and prosthesis models in Studies I, II and IV.

	N	Prosthesis model
Study I	123 patients (130 ankles)	130 AES
Study II	40 patients (42 ankles)	42 AES
Study IV	32 patients (34 ankles)	31 AES, 3 STAR

AES, Ankle Evolutive System (Biomet, Warsaw, Indiana, USA)
STAR, Scandinavian Total Ankle Replacement (Waldemar Link, Hamburg, Germany)

Between 2002 and 2008, altogether 123 patients (130 ankles) received an Ankle Evolutive System (AES; Biomet, Warsaw, Indiana, USA) TAA in our hospital. The operations were performed under spinal or general anesthesia through a straight midline anterior incision. A tourniquet was not used. Postoperatively, patients were immobilized in a cast for 6 to 8 weeks and they were allowed full weight-bearing from the beginning. After cast removal normal, unrestricted walking was allowed. In Study I, radiographs of all patients were evaluated. There were 45 males and 78 females; their mean age at operation was 56.4 years (range, 18-86 years). Of the patients 68 patients (73 ankles) had osteoarthritis, 50 patients (52 ankles) rheumatoid arthritis, and 5 had other diagnosis (3 psoriatic arthropathies, one

reactive arthritis, and one congenital anomaly). 16 ankles of 130 ended up in being reoperated due to periprosthetic osteolysis.

Of these 123 patients (130 ankles), 43 had at least one large (diameter greater than 10 mm) osteolytic lesion on radiographs. 40 patients (42 ankles) of 43 were recruited for Study II. 3 patients were excluded because of not having a CT follow-up of the ankle. Both CT and radiographs were evaluated in Study II. There were 21 males and 19 females; their mean age at operation was 56.3 years (range, 33-76 years). 25 patients had osteoarthritis, 13 rheumatoid arthritis, and 2 patients had other diagnosis. Their mean body mass index was 28 kg/m^2 (range, 19-47 kg/m^2).

In Study IV we studied all patients who had undergone a reoperation due to periprosthetic osteolysis following TAA with Scandinavian Total Ankle Replacement (STAR; Waldemar Link, Hamburg, Germany) or AES total ankle replacement. The first 3rd generation TAA was performed in the Turku University Hospital in 1997. The first prosthesis model was the STAR, which was later replaced by the AES. STAR and AES prostheses operations were performed between 1997 and 2008. The total amount of prostheses was 164 (34 STAR and 130 AES). 46 of these 164 ankles (44 patients) ended up in a reoperation due to periprosthetic osteolysis. Twelve patients did not have medium-term follow-up by CT after reoperation, and thus 34 ankles (32 patients) were finally included in Study IV. The reoperations of these 34 ankles (32 patients) were performed between 2008 and 2010. In all reoperations the metallic components were left firmly in place, i.e., tibial or talar components were not removed. One to 3 osteolytic lesions in each ankle were grafted. Data of the reoperations is presented in Table 2. There were 19 male and 13 female patients, whose mean age was 60.4 years (range, 36-78 years) at the time of reoperation. The preoperative diagnosis was osteoarthritis in 22 patients and rheumatoid arthritis in 10 patients. The mean body mass index at the primary operation was 29 kg/m^2 (range, 20-47 kg/m^2). 3 patients had a STAR ankle prosthesis and 29 patients (31 ankles) an AES prosthesis.

4.3.   Animals (Study III)

In Study III we used an AES total ankle prosthesis in a dissected pig's knee joint to create a model for ankle prosthesis. The size of the pig's knee corresponds quite well to the human ankle. An orthopedic surgeon experienced in ankle arthroplasty operations installed the prosthesis in the joint; soft tissues and skin were left around the joint. To improve the fitting of the prosthesis components, the bones of the knee joint were turned 'upside down' so that the talar component was placed in the femoral trochlea and the tibial component in the proximal head of tibia. Four defects of different size were drilled around the prosthesis components, simulating

Table 2. Data of the reoperations (number of ankles, n = 34). (Original publication IV).

	Number	%
Bone graft	34	
Allograft	29	85
Autograft	4	12
Both	1	3
Polyethylene component changing	34	
Yes	24	71
No	10	29
BMP (bone morphogenetic protein) -7	34	
Yes	5	15
No	29	85
Attendance in reoperation	34	
Orthopaedic surgeon no 1 (H.T)	21	68
Orthopaedic surgeon no 2	16	47
Orthopaedic surgeon no 3 (H.K)	6	18
Orthopaedic surgeon no 4	1	3
Orthopaedic surgeon no 5	5	15
Medical treatment	34	
Bisphosphonate (tsoledronic acid)	9	26
Denosumab	6	18
Both	16	47
No medical treatment	3	9

periprosthetic osteolytic lesions. A 1 ml syringe with water was used in measuring the sizes of these defects. The defects around the tibial component were 0.55 and 2.1 ml and around the talar component 0.5 and 1.5 ml. During scanning the drilled defects around the prosthesis were filled with low-fat ground meat (percentage of fat under 10%) to simulate granulomas and avoid air in them.

4.4.   Prosthesis models

The Ankle Evolutive System, AES (Biomet, Warsaw, Indiana, USA) is a 3-piece uncemented, unconstrained design with tibial and talar components of cobalt-chromium (Co-Cr). It has a front-to-back mobile bearing of ArCom (Biomet, Warsaw, Indiana, USA) ultra-high molecular weight polyethylene (UHMWPE) between the flat tibial component and the shallow sulcus of the talar implant. In 2004, the design was changed from Co-Cr components with a hydroxyapatite (HA) coating to a porous coating of pure titanium with an HA coating (dual-coated; Ti-HA). The tibial component was also changed from a modular stem to a monoblock. The prosthesis model in Studies I and II was the AES. The TAA of the pig in Study III was also AES. In Study IV the most common implant type was AES.

The Scandinavian Total Ankle Replacement, STAR (Waldemar Link, Hamburg, Germany), consists of three components: tibial and talar components of cobalt-chromium (Co-Cr) and an ultra-high molecular weight polyethylene (UHMWPE) gliding core. The tibial component has a highly polished flat articulation surface and two cylindrical fixation bars which attach the implant to the tibia. The talar component has a ridge running anteroposteriorily in the middle of the gliding surface guiding the polyethylene gliding core. A porous plasma spray of dual-coating (Ti-CaP) is applied to the STAR TAA. In Study IV there were 3 STAR prostheses.

4.5.   Methods

4.5.1.   Imaging protocols

4.5.1.1. Radiographs (Studies I, II)

In Study I, the radiographs of 123 patients (130 ankles) were studied. Anteroposterior (AP) and lateral radiographs of the ankle were taken standing, whenever possible. Radiographs of ankles were taken preoperatively and at 6 weeks, at 2 or 3 months, and at 1 year, 2 years, and 3 years after the operation.

In Study II, the radiographs of 40 patients (42 ankles) with at least one large (diameter over 10 mm) periprosthetic osteolytic lesion were evaluated. Anteroposterior and lateral radiographs of ankle were taken at 6 weeks, 2 or 3 months, and 1 year, 2 years, and 3 years after the operation.

4.5.1.2. Computed tomography (Studies II-IV)

In Study III, the pig's knee with the AES implant was CT-imaged with a Siemens Somaton Sensation 64-slice CT (Siemens AG Healthcare Sector, Erlangen, Germany). The joint with the prosthesis was imaged in four different orientations: the tibial stem parallel to the table and at 25, 45, and 90° angles to it. The talar component alignment remained unchanged in relation to the x-ray tube. The specimen with the implant was in a cardboard box during scanning. A wooden stick was fixed to the tibial component. With the fixed stick and holes in one wall of cardboard box the tibial component could be rotated in different angles to the table, while the talar component alignment remained unchanged when scanning the prosthesis model on CT. The protocol consisted of scanning at 100, 120, and 140 kVp in every angle with a pitch of 1.2. The scanning at 120 kVp in every angle was repeated with a pitch of 1.0. Beam hardening and metal-artifact-minimizing algorithms and tube current modulation were used. The slice thickness was 0.6 mm and the reconstruction increment was 0.4 mm.

In Study II, 40 patients (42 ankles) with at least one large (diameter over 10 mm) radiographic periprosthetic osteolytic lesion, CT images were obtained using Siemens Somatom Sensation 64-slice CT (Siemens AG Healthcare Sector, Erlangen, Germany). The protocol consisted of scanning at 120 kV with a metal-artifact-minimizing algorithm. Automatic tube current modulation was used. The slice thickness was 0.6 mm and the reconstruction increment was 0.4 mm. Patients were supine during scanning. The scanned area included the whole implant (stretching from the proximal end of the tibial component to the subtalar joint).

In Study IV, 32 patients (34 ankles) with medium-term follow-up after reoperation due to TAA osteolysis were examined by CT, which was done before reoperation, immediately after reoperation, and approximately once a year after reoperation. A Siemens Somatom Sensation 64-slice CT was used (Siemens AG Healthcare Sector, Erlangen, Germany). The protocol consisted of scanning at 120 kV with a metal-artifact-minimizing algorithm based on the extended CT-scale technique. Automatic tube current modulation was used. The slice thickness was 0.6 mm and the reconstruction increment was 0.4 mm. The scanned area included the whole implant stretching from the proximal part of the tibial component to the subtalar joint. During scanning, patients lied supine with their knees straight on a table.

4.5.2. Histological and microbiological samples (Study I)

In Study I, 16 ankles out of 130 were reoperated for periprosthetic osteolysis. All ankles had been fitted with an AES TAA, and out of them, 7 had a porous Ti-HA coating and 9 a HA coating. At reoperation samples were taken from the osteolytic cavities, the joint capsule, and the joint fluid for microbiological and histological analyses.

4.5.3. Data analysis

4.5.3.1. Radiographs (Studies I, II)

In Study I, radiographs of 123 patients (130 ankles) were evaluated by 2 independent observers: one orthopedic surgeon and one radiologist. The main purpose was to detect possible osteolytic lesions around the prosthesis components. To be able to exclude degenerative cysts and geodes, the preoperative radiographs were also reviewed. The observers were blinded to which type of AES implant had been used, a porous Ti-HA coating or a HA (hydroxyapatite) coating. Conclusions were made by consensus. The longest diameter of any osteolytic lesion was measured using the Kodak Carestream PACS system software (Carestream Health, Rochester, NY). Osteolysis was defined as a discrete, well-circumscribed area of lucency at least 2 mm wide in the periprosthetic bone, and radiolucency as a completely radiolucent
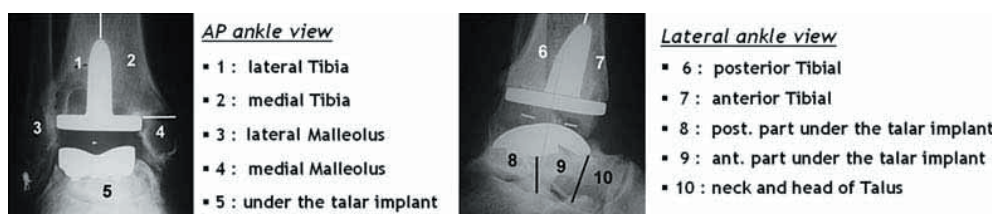
Figure 2. Radiographs showing the zones (1-10) around the Ankle Evolutive System prosthesis and classification of lesions (according to Besse et al. 2009). Each zone was classified as follows: N (normal), L (lucency, less than 2 mm), cyst A (2-5 mm), cyst B (5-10 mm), cyst C (10-20 mm), cyst D (20-30 mm), and cyst E (greater than 30 mm). (Original publication II).

line less than 2 mm in width at the bone-implant interphase. The periprosthetic area was divided into 10 zones according to Besse (Besse et al. 2009), the tibial component into 6 zones and the talar component into 4 zones. The osteolytic lesions were classified by size, and lesions greater than 10 mm (Cysts C to E) were considered to be major (Figure 2). Implant migration was assessed by comparing radiographs taken immediately after operation with the radiographs at the most recent follow-up. Also, substantial medial or lateral overhang between the tibial and talar component in the AP view was examined. If it was 3 mm or greater, the polyethylene insert was considered to protrude beyond the edge of the metallic component. Both migration of the implant and substantial overhang were evaluated by one observer.

In Study II, the radiographs of 40 patients (42 ankles) were studied by 2 independent observers: one orthopedic surgeon not involved in the surgeries and one radiologist with 3 years of experience in musculoskeletal radiology. The observers were blinded to which type of AES implant had been used. Conclusions were drawn by consensus. The osteolytic lesions were measured as in Study I; the longest diameter of the lesion was measured. The tibial component was divided into 6 zones and the talar component into 4 zones as in Study I. The osteolytic lesions were classified by size, and lesions greater than 10 mm were considered to be major. The Kodak Carestream PACS system software (version 10.2; Carestream Health, Rochester, NY) was used. The mean time interval between the radiographs and the following CT was 5.6 months (range, 0-23 months).

4.5.3.2. CT (Studies II-IV)

In Study III, one prosthesis model was imaged on CT in different orientations using different imaging parameters. In the pig experiment, the volumes of the drilled defects around the prosthetic components were measured by a volumetric analysis tool provided by syngo MultiModality Workplace (VE 36A, Siemens AG Healthcare Sector, Erlangen, Germany). The streak artifacts caused by metallic prosthesis

components were visually assessed. The volume measurements were done twice by 1 radiologist with 5 years of experience in musculoskeletal radiology. There were approximately 11 months between the two measurement sessions. The radiologist was not blinded to the imaging parameters when interpreting the data.

In Study II, the 42 ankles of 40 patients underwent CT. Each ankle had at least one major periprosthetic osteolytic lesion by radiography. Coronal, sagittal, and axial images (in relation to the tibial implant) were reformatted from the original data. Measurements on CT images followed the same orientations as the ankle radiographs (coronal and sagittal projections). A similar zoned system was used as for radiographic analysis (see section 4.5.3.1.). The area surrounding the ankle prosthesis was divided into 10 zones according to Besse et al. (2009). To make radiographic and CT methods comparable, the osteolytic lesions were classified by size in a similar way. For example, in zone 6, the slice with the largest osteolytic lesion from sagittal images was chosen and the longest diameter of the lesion was measured. CT images were analyzed by 2 independent radiologists, both with 3 years of experience in musculoskeletal radiology. Conclusions were made by consensus. The Kodak Carestream PACS system software (version 10.2; Carestream Health, Rochester, NY) was used. The mean time interval between primary operation and CT was 48.7 months (range, 19-86 months).

In Study IV, coronal, sagittal, and axial images (in relation to the tibial implant) were reformatted from the original CT data of 32 patients (34 ankles). The volume measurements of the osteolytic lesions were done using Aycan Workstation Osirix [pro] (version 1.04; Wurzburg, Germany). The streak artifacts caused by metallic ankle prosthesis were visually assessed. Intraobserver reliability was evaluated by repeated volume measurements after reoperation by one musculoskeletal radiologist. The time between the evaluations was 5 months. For interobserver reliability evaluation, this evaluation was made once by another musculoskeletal radiologist. Postoperative volume measurements were done at 3 different time points: immediately after reoperation, 1 year after the reoperation, and the most recent follow-up available. The mean CT follow-up after reoperation was 3.8 years (range, 2.0-6.2 years). If the patient underwent ankle arthrodesis or repeated bone grafting (rereoperation), this was considered as the end point of the CT follow-up. The preoperative volume measurements of the osteolytic lesions were performed once by one observer.

4.5.3.3. Histological and microbiological samples (Study I)

For histological analyses the samples were fixed in formalin and stained with the hematoxylin-eosin and van Gieson stains. Serial sections 4 μm to 10 μm were

made from paraffin-embedded specimens. The samples were examined by light and polarized-light microscopy. Backscattered electron imaging with a scanning electron microscope (BEI-SEM) (Leo Gemini 1530; Carl Zeiss SMT AG, Jena, Germany) equipped with energy dispersive radiographic (EDX) analysis was performed on histological samples with debris particles under light microscopy. The sample surface was coated with a thin layer of carbon. The EDX analysis was used for identification of the elements.

For analysis of the elements in the periprosthetic tissue, the samples were dried to constant weight and the organic material of the bone samples were destroyed with a mixture of nitric, sulphuric, and chloral acids (perchloric). The analyses were performed with the ICP-MS technique (Thermo XSeries2 ICP-MS, Thermo Electron Corporation, Waltham, Massachusetts, equipped with a collision reaction cell). Germanium, platinum, and scandium group metals were used as internal standards. It is based on the NIOSH 7000 series methods (NIOSH Manual of Analytical Methods). The standards were made in acidified solutions, and for rare elements a semi-quantitative method was used. The detection limit for the elements analyzed was at least < 0.0001 mg/g.

4.5.4. Statistical methods

In Study I, statistical calculations were made with the SPSS software (version 16.01; SPSS Inc., Chicago, Illinois, USA). Survivorship curves with periprosthetic osteolysis as the endpoint were drawn with the Kaplan-Meier method. Implants were compared with the log-rank test. Cox's proportional hazards model was used to analyze whether the type of implant or any demographic factors influenced the risk of osteolytic lesions. A p-value of < 0.05 was considered statistically significant.

In Study II, the significance of the differences of the sizes of the periprosthetic osteolytic lesions between radiographs and CT was assessed with Wilcoxon's signed rank test. The Mann-Whitney U test was used to compare the sizes of the osteolytic lesions between HA-coated implants and dual-coated (Ti-HA) implants, in males and females and in different diagnosis groups. Spearman's correlation coefficients were calculated to describe the relationships between age and osteolysis on CT and between BMI and osteolysis on CT. The statistical analyses were made with the SAS System for Windows (version 9.2; SAS Institute Inc., Cary, NC, USA). P < 0.05 was considered to be statistically significant.

In Study III, analysis in variance was used to evaluate the effect of orientation of the ankle prosthesis, the tube voltage, and the pitch on artifacts caused by the metal implant. The effects of tube voltage and angle, i.e., orientation of the tibial component, were adjusted for the component. Tukey's adjustment method was

used in further pairwise comparisons with analysis of variance. The intraclass correlation between the first and second measurement sessions was calculated to test for the reliability of the measurements. The limits of agreement between the first and second measurement sessions were quantified with the Bland-Altman plot. The statistical analyses were performed with the SAS System for Windows (version 9.2; SAS Institute Inc., Cary, NC, USA). A level of significance of $\alpha = 0.05$ was used.

In Study IV, binary logistic regression was used to analyze the associations among the demographic parameters of the population with respect to the appearance of osteolytic lesion among patients with constant bone grafting during the follow-up period. Linear models were used to test for the associations among the demographic parameters with regard to progression of osteolysis during follow-up. Since the progression values had a positively skewed distribution, data were log-transformed. Generalized estimation equations were used to account for the correlation between lesions measured on the same patient. Intraclass correlation coefficients were calculated to test for intraobserver and interobserver reliability. P-values < 0.05 were considered to be statistically significant. Statistical analyses were done with the SAS System for Windows (version 9.4; SAS Institute Inc., Cary, NC, USA).

5.   RESULTS

5.1.   Periprosthetic osteolysis and total ankle arthroplasty (Study I)

Osteolytic lesions and radiolucent lines were seen in 48 radiographs of 130 ankles (37%) during a mean follow-up of 31.3 months (range 3-74 months). Of these, only 2 patients had isolated radiolucent lines at the bone-implant interphase, while all the others had osteolytic lesions. Major (diameter over 10 mm) osteolytic lesions were identified on the radiographs of 27 ankles (21%); 26 of these ankles were imaged with CT. By radiography (AP and lateral projections), the most common site of lesions was around the tibial stem. The impression was that there were more osteolytic lesions in the talus on CT images than radiographs. However, the CT images were not systematically evaluated in this sub-study. During follow-up, the osteolytic lesions of 16 ankles (33%) progressed by radiography.

The risk for osteolysis was 3.1 (95% CI 1.6 to 5.9) times higher for dual-coated (Ti-HA) implants than for implants with HA coating alone (p = 0.001) (Figure 3). Male patients had 2.0 (95% CI 1.13 to 3.6) times higher risk for osteolysis (p = 0.018) than female patients, but a statistically significant correlation was not found for major osteolysis (p = 0.08). None of the other demographic factors, including age (0.47, p = 0.82), diagnosis (1.00, p = 0.92), bisphosphonate therapy (0.68, p = 0.88), or anti-TNF therapy (0.11, p = 0.44) were significant risk factors.

Substantial overhang was detected in 9 ankles; in three cases with osteolysis. This finding was not statistically significant (p = 0.21) risk for osteolysis. The talar component migrated in 9 ankles (7%) and in 2 of these ankles a shift of the tibial component was found as well. The factors predisposing to talar component migration were: osteolysis (n = 4), talar necrosis (n = 2), deep infection with talar necrosis (n = 1), neuropathic arthropathy (n = 1), and no specific reason (n = 1). Tibial component migration occurred only in 2 ankles. The migration of 1 tibial component was minimal and was associated with migration of the talar component due to osteolysis. In 1 patient who experienced migration of the tibial component, there was osteolysis around the tibial component.

At reoperation, 15 out of 16 patients had major periprosthetic osteolysis in the tibia and/or talus, while 1 patient had large osteolytic lesion in the lateral malleolus. The patient with the large osteolytic lesion in lateral malleolus underwent debridement and allografting. There was no bacterial growth in the samples and histological examination showed mostly fibrosis, with no apparent foreign-body reaction or presence of wear particles. In the other ankles the large cavities around the prosthesis components contained brownish-grey, granulomatous, necrotic material with no
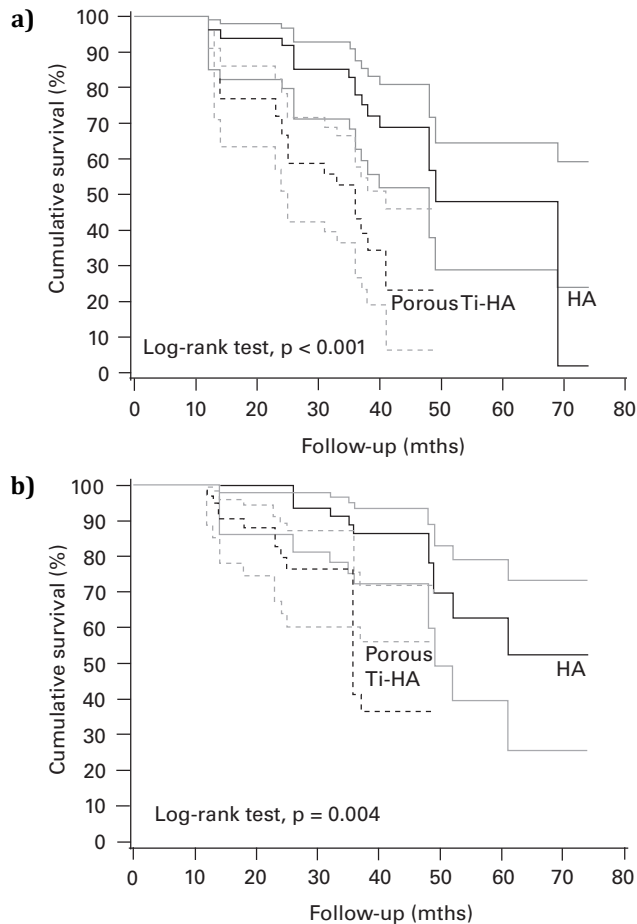
Figure 3. Kaplan-Meier survival curves of implants with osteolysis as the endpoint showing **a)** osteolytic lesions and **b)** major lesions (HA, hydroxyapatite; Ti-HA, titanium hydroxyapatite). Grey lines indicate 95 % confidence intervals. (Original publication I).

visible metallosis in the surrounding structures. In 12 of the ankles both metallic prosthesis components were stable when tested during operation. Debridement of the lesions and grafting with allogenous cancellous bone was carried out in all cases, and also the polyethylene component was changed. In 3 ankles with HA coating one of the metallic components was loose and arthrodesis was done. All the polyethylene components appeared intact when examined during operation. The osteolytic sites were sterile, as shown by negative bacterial cultures and staining. In most of the histological samples large acellular, necrotic areas were seen, but wear debris was absent. There was an increased number of histiocytes containing small, sharp particles of foreign material seen best under polarized light. A few giant cells were also present. The number of osteoclasts was increased compared to normal bone tissue. There were also sporadic lines of resorption in the healthy bone tissue. The histological findings were largely compatible with a foreign-body reaction.

Table 3. Number of patients and distribution in percentages in different zones and classes. The biggest group in each zone is in bold type. (Original publication II).

	N	L	A	B	C	D	E
Zone 1							
RG	9 (21.4)	0	4 (9.5)	8 (19.1)	**15 (35.7)**	5 (11.9)	1 (2.4)
CT	2 (4.8)	0	1 (2.4)	10 (23.8)	**23 (54.8)**	5 (11.9)	1 (2.4)
Zone 2							
RG	**14 (33.3)**	0	6 (14.3)	10 (23.8)	7 (16.7)	3 (7.1)	2 (4.8)
CT	9 (21.4)	0	2 (4.8)	6 (14.3)	**17 (40.5)**	7 (16.7)	1 (2.4)
Zone 3							
RG	**35 (83.3)**	0	0	2 (4.8)	2 (4.8)	3 (7.1)	0
CT	**23 (54.8)**	0	1 (2.4)	8 (19.1)	8 (19.1)	2 (4.8)	0
Zone 4							
RG	**30 (71.4)**	0	0	7 (16.7)	5 (11.9)	0	0
CT	**22 (52.4)**	0	2 (4.8)	2 (4.8)	15 (35.7)	1 (2.4)	0
Zone 5							
RG	**36 (85.7)**	0	1 (2.4)	1 (2.4)	4 (9.5)	0	0
CT	3 (7.1)	0	0	11 (26.2)	**23 (54.8)**	3 (7.1)	2 (4.8)
Zone 6							
RG	10 (23.8)	0	3 (7.1)	5 (11.9)	**22 (52.4)**	2 (4.8)	0
CT	2 (4.8)	0	2 (4.8)	7 (16.7)	**23 (54.8)**	7 (16.7)	1 (2.4)
Zone 7							
RG	12 (28.6)	0	4 (9.5)	5 (11.9)	**18 (42.9)**	2 (4.8)	1 (2.4)
CT	5 (11.9)	0	1 (2.4)	5 (11.9)	**26 (61.9)**	4 (9.5)	1 (2.4)
Zone 8							
RG	**41 (97.6)**	0	0	1 (2.4)	0	0	0
CT	**19 (45.3)**	0	0	6 (14.3)	17 (40.5)	0	0
Zone 9							
RG	**29 (69.1)**	0	2 (4.8)	7 (16.7)	4 (9.5)	0	0
CT	7 (16.7)	0	0	6 (14.3)	**21 (50.0)**	6 (14.3)	2 (4.8)
Zone 10							
RG	**38 (90.5)**	1 (2.4)	0	1 (2.4)	2 (4.8)	0	0
CT	**33 (78.6)**	0	1 (2.4)	1 (2.4)	7 (16.7)	0	0

Note: N, normal; L, lucency (less than 2 mm); A, bone lysis between 2 and 5 mm; B, bone lysis between 5 and 10 mm; C, bone lysis between 10 and 20 mm; D, bone lysis between 20 and 30 mm; E, bone lysis greater than 30 mm. Abbreviations: RG, radiograph; CT, computed tomography.

The BEI-SEM/EDX analysis of samples from porous Ti-HA ankles revealed several micrometer-sized particles of titanium and Co-Cr. Polyethylene particles were not identified. There were measurable amounts of titanium, chromium, cobalt, aluminium, and molybdenum in the Ti-HA samples. The amount of Ti was 230 µg/g of dry tissue, of Cr 18, of Co 11, of Al 1.7, and of Mo 1.2 µg/g of dry tissue.

5.2. Radiographs vs. CT for detecting osteolysis around TAA (Study II)

165 osteolytic lesions were detected in different zones on radiographs and 295 on CT in 40 patients (42 ankles). The number of major lesions (diameter over 10 mm) was 98 on radiographs and 222 on CT. Class N (normal) was the most common group in
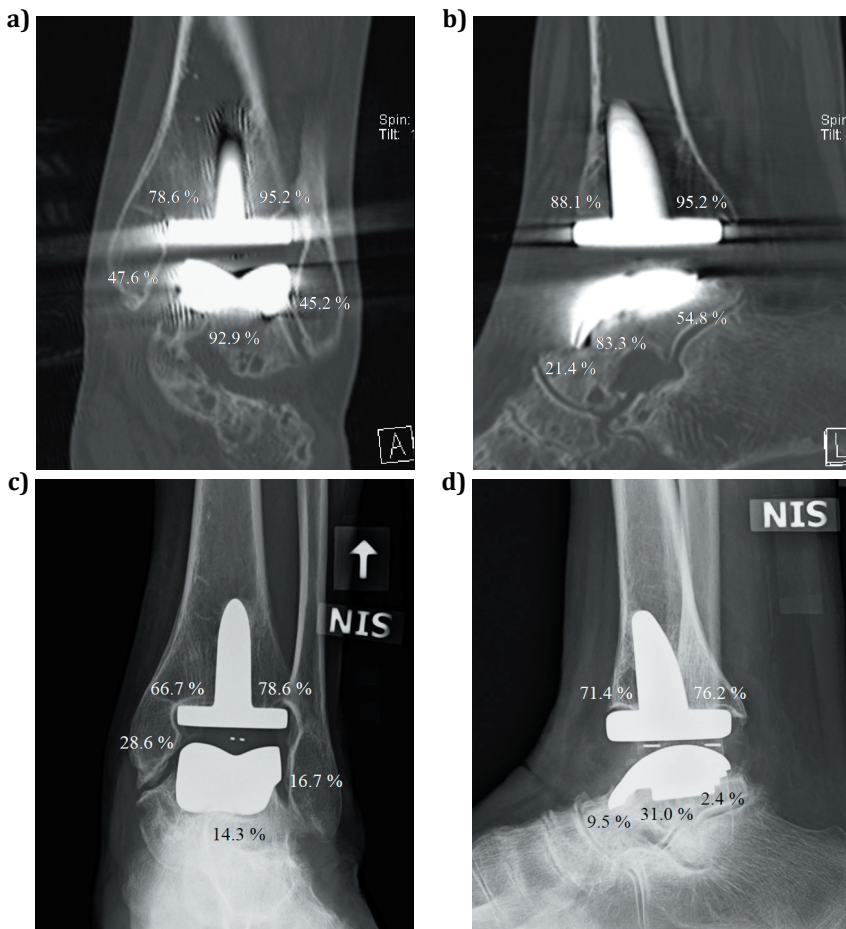
Figure 4. Distribution of all osteolytic lesions in percentages in different zones on CT (**a**, **b**) and on radiographs (**c**, **d**). (Original publication II).

zones 2, 3, 4, 5, 8, 9, and 10 on radiographs but only in zones 3, 4, 8, and 10 on CT. Class C (osteolysis between 10 and 20 mm) was the most common group on CT images in all the other zones: 1, 2, 5, 6, 7, and 9. Class C was the most common group only in zones 1, 6, and 7 on radiographs. Only once was lucency (lytic line less than 2 mm wide) detected in zone 10 on radiographs; all the other lesions were osteolytic (lytic area 2 mm wide or greater) (Table 3, Figure 4). Osteolytic lesions were larger in all zones on CT compared with radiographs. The difference was statistically significant in 9 of 10 zones (zone 1, p = 0.0002; zone 2, p = 0.0025; zone 3, p = 0.0012; zone 4, p = 0.0046; zone 5, p < 0.0001; zone 6, p = 0.0002; zone 7, p = 0.0004; zone 8, p < 0.0001; zone 9, p < 0.0001; zone 10, p = 0.0703). The difference was highly significant in zones 5, 8, and 9 (p < 0.0001) on the side of the talus (Figure 5).

There was no significant difference between the size of the osteolytic lesions on CT with respect to the design of the AES prosthesis (HA coated and Ti-HA coated), gender, diagnoses, age, or BMI.
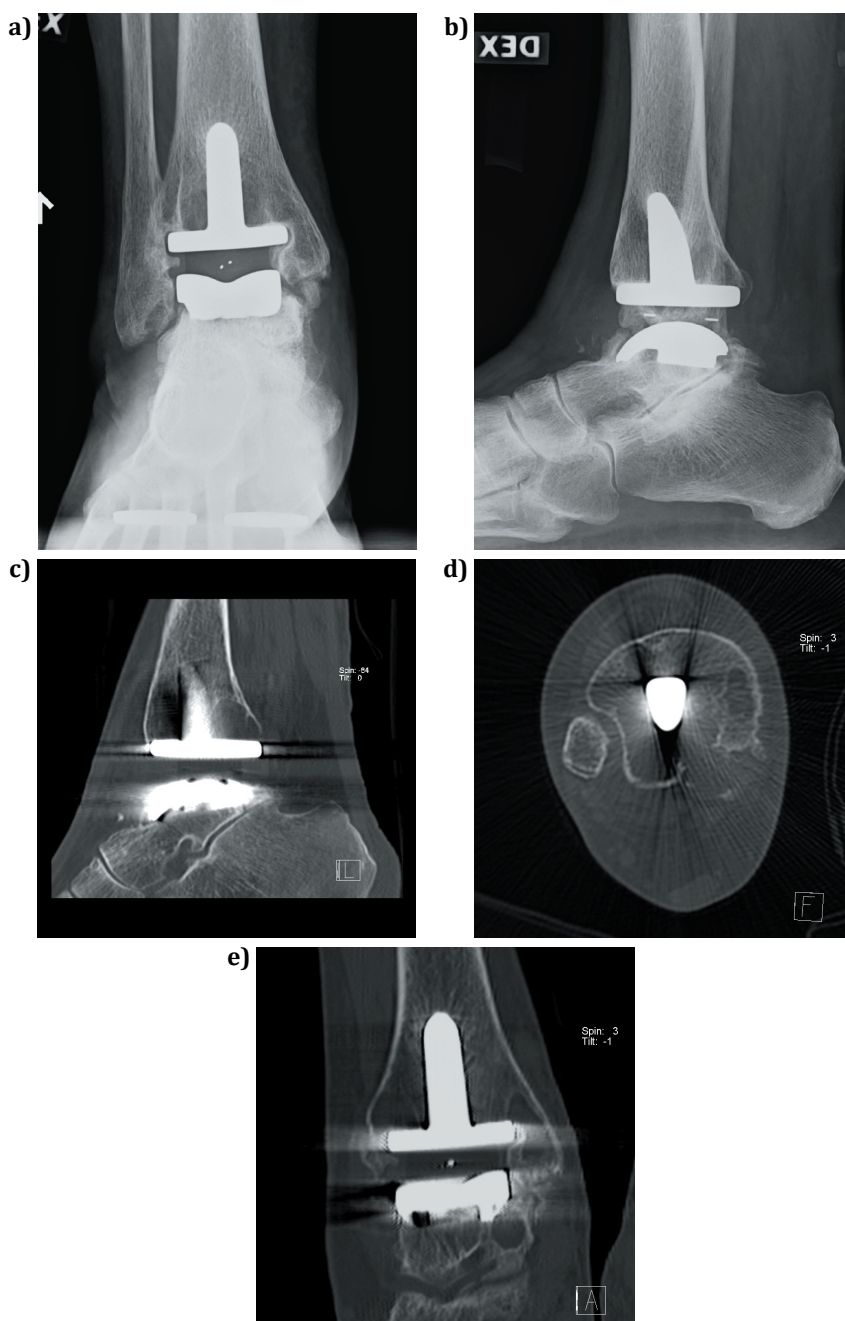
Figure 5. Images of a 73-year-old woman with rheumatoid arthritis in ankle. Radiographs (**a**, **b**) 3 years and 9 months after total ankle arthroplasty and CT images (**c**, **d**, **e**) 4 months after radiographs. There is an expansive osteolytic lesion and cortical disruption dorsal to the tibial stem. There are osteolytic lesions also in medial malleolus and under medial margin of the talar component; seen only on CT images (5e).

Table 4. Volume measurement differences (measured volumes minus real volumes) with a pitch of 1.2. Angle means the alignment of tibial stem to table. Mean difference is tube voltage and component adjusted. (Original publication III).

Angle (degrees)	Mean difference (ml)	SE (ml)	p value*
0	0.01	0.07	0.89
25	-0.34	0.07	< 0.0001
45	-0.58	0.11	< 0.0001
90	-1.30	0.13	< 0.0001

SE standard error

* Analysis of variance; Tukey's method was used in pairwise comparisons.

5.3. Effect of orientation and imaging parameters on metal artifacts on CT (Study III)

There were no significant differences between the measured and the real volumes (measured volumes minus real volumes) of the defects (n = 4) in the prosthesis model when the tibial stem was parallel to the table during scanning with a pitch of 1.2. When the tibial stem was at 25°, 45°, and 90° angles to the table, there were statistically significant differences between the volume measurements on CT and the real volumes (p values in all < 0.0001) (Table 4). During the first measurement session the means and standard deviations (SD) were as follows: 0.02, 0.17 (0°); -0.30, 0.22 (25°); -0.52, 0.58 (45°) and -1.28, 0.26 (90°). A scatter plot shows the differences between the measurements on CT images and the real volumes (Figure 6). The smaller defects around both the tibial and the talar components could not be detected at all, regardless of tube voltage because of increased artifacts caused by metallic components when the tibial stem was at 45 and 90° angles to the table.
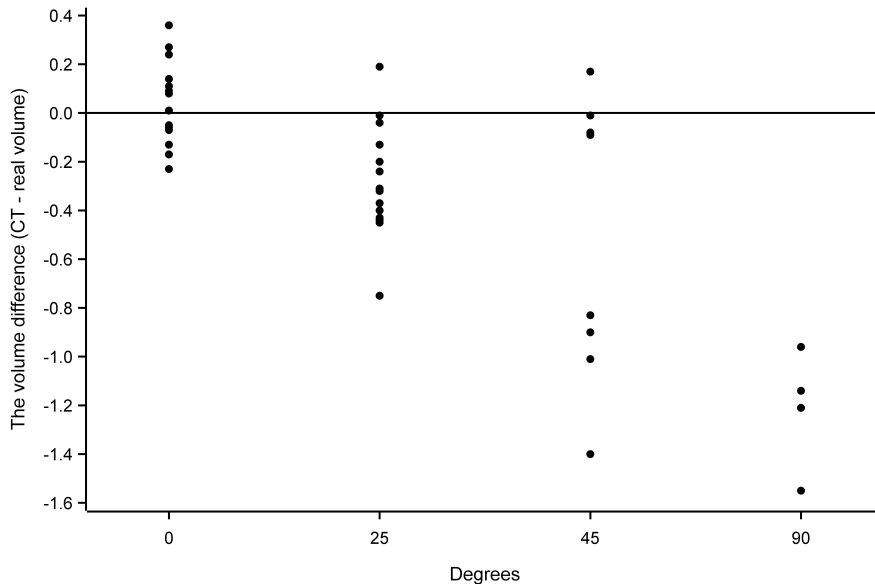

Figure 6. Scatter plot displays the differences between the measured and real volumes (ml) according to degrees during the first measurement session (0°: min -0.23, max 0.36; 25°: min -0.75, max 0.19; 45°: min -1.4, max 0.17; 90°: min -1.55, max -0.96). (Original publication III).
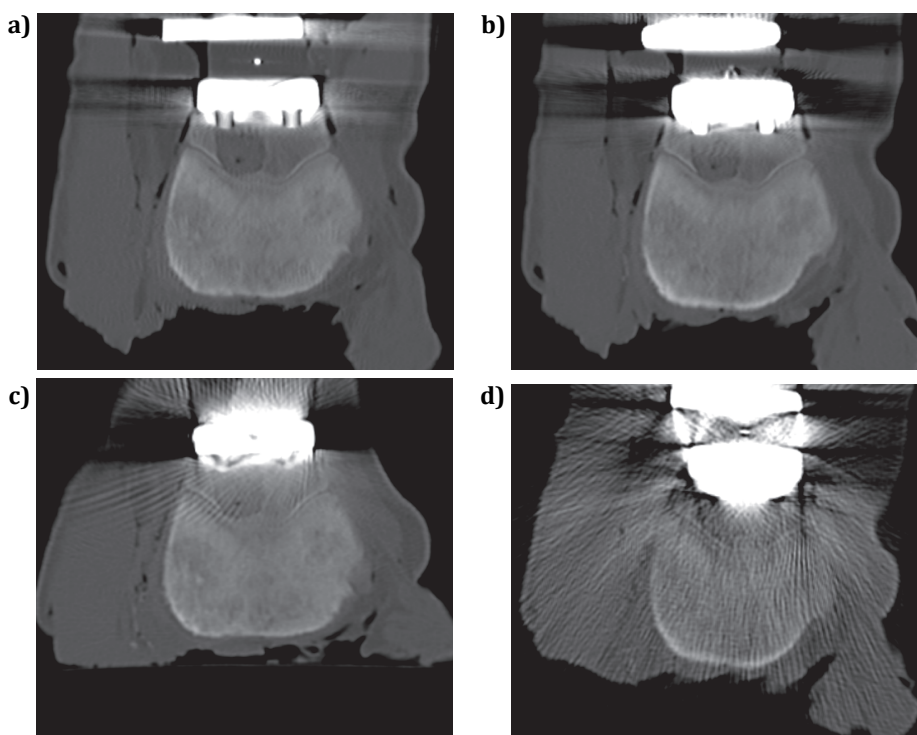
Figure 7. CT, coronal slices through the larger defect under the talar component. The larger defect under the talar component is shown on images obtained with the tibial stem parallel to the table (**a**) and at 25 and 45° angles (**b**, **c**) to it. The defect is not detectable due to increasing artifacts on images obtained with the stem at a 90° angle (**d**) to the table. All images are taken with 120 kV and a pitch of 1.2. (Original publication III).

Volume measurements of the defects with a pitch of 1.2 were significantly different between the angles (0°, 25°, 45°, 90°) in each comparison (p < 0.0125 or lower in all pairwise comparisons), except one, between 25° and 45°.

In the whole data set with a pitch of 1.2 there were no statistically significant differences between different tube voltages (100, 120, and 140 kVp) regarding volume measurements (adjusted for angle and component, p = 0.24). However, when the tibial stem was at a 90° angle to the table, the bigger defect around the talar component could not be detected at all because of major artifacts when scanning at 100 kVp and 120 kVp (Figure 7). When scanning at 140 kVp and 90° angle the bigger defect around the talar component could be partially identified despite the artifacts. Volume measurement differences between 2 pitch-values, 1.0 and 1.2, did not differ significantly when scanning at 120 kVp (angle adjusted p = 0.43).

The intraclass correlation of the measurement differences between the first and second measurement sessions was 0.96, i.e., repeatability is excellent. The limits of agreement between the first and second volume measurement session differences were from -0.28 to 0.28 ml.
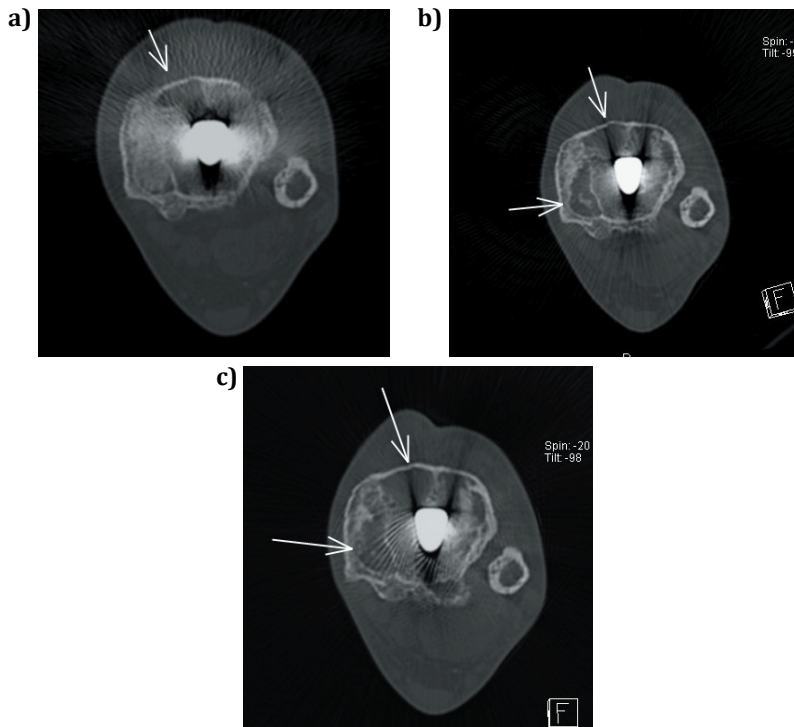
Figure 8. CT images of a 59-year-old man with rheumatoid arthritis in ankle. An axial slice (**a**) of osteolytic lesions medial and anterior to tibial stem immediately after bone grafting. The grafting result is good medially, anteriorly there is a small residual lesion. Axial slices one year (**b**) and four years (**c**) after reoperation; there are enlarging recurrent lesions in both areas. Arrows indicate residual/recurrent lesions. (Note bigger metal artifacts in the first image compared to other images; the first image has been taken from the patient with flexed knees. The second (**b**) and third (**c**) images have been taken with straight knees.)

5.4. CT for follow-up of bone-grafted osteolytic lesions around TAA (Study IV)

Altogether 65 osteolytic lesions around TAAs were grafted in 34 ankles (32 patients). The median volume of the osteolytic lesion before reoperation was 1.34 ml measured by CT (IQR, 0.63-2.58). In 44 bone-grafted periprosthetic areas (68%) there was radiographic progression during the follow-up period (immediately after reoperation vs. most recent follow-up). In 38 bone-grafted areas (58%) there was progression during the first year after reoperation. Of these, 28 osteolytic lesions continued to enlarge also during the next follow-up period (one year after reoperation vs. most recent follow-up). In 18 bone-grafted lesions (28%) there was no residual or recurrence cavity on CT during the entire follow-up.

Of 48 bone-grafted areas with no residual lesion immediately after reoperation 30 (63%) had a recurrent osteolytic lesion during follow-up. In 17 areas there was postoperatively residual osteolytic lesion with a median volume of 0.23 ml (IQR, 0.12-0.71). Of these 17 residual osteolytic lesions, 14 (82%) continued to grow

Table 5. Demographic parameters for progression of osteolytic lesions in the follow-up period (number of lesions with progression, n = 44). (Original publication IV).

	n	Estimate	Mean* (ml)	Median (ml)	IQR (interquartile range)	p-value
Pain	44					0.043
Pain 1 (1 = painless)	22	-0.283	0.75	0.76	0.37-1.38	0.49[1]
Pain 2+3 (2 = starting pain, 3 = sometimes pain when loading)	16	-0.606	0.55	0.45	0.29-1.26	0.27[2]
Pain 4+5 (4 = always pain when loading, 5 = pain at rest)	6	-1.187	0.31	0.31	0.19-0.48	0.034[3]
Function (no data from 6 lesions)	38					0.079
Function 1+2 (1 = notably better, 2 = little better)	35	-0.54	0.58	0.48	0.30-1.38	
Function 3+4 (3 = no change, 4 = worse)	3	-0.138	0.87	0.79	0.65-1.28	
Graft type	44					0.054
Allograft	36	-0.619	0.54	0.47	0.29-1.07	
Autograft+1 patient auto- and allograft	8	-0.076	0.93	0.87	0.38-1.64	
Diagnosis	44					0.945
Rheumatoid arthritis	14	-0.506	0.60	0.56	0.36-1.01	
Osteoarthritis	30	-0.531	0.59	0.54	0.30-1.28	
Sex	44					0.165
Men	25	-0.35	0.70	0.71	0.34-1.28	
Women	19	-0.734	0.48	0.44	0.28-1.01	
Age	44					0.361
Under 50 years	8	-0.329	0.72	0.56	0.35-1.32	
Over 50 years	36	-0.561	0.57	0.54	0.29-1.19	
BMI (body mass index)	44					0.117
BMI <30	20	-0.277	0.76	0.66	0.38-1.64	
BMI >30	24	-0.701	0.50	0.41	0.27-1.07	
Size of the lesion	44					0.323
Under 2 ml	19	-0.687	0.50	0.59	0.32-1.28	
Over 2 ml	25	-0.408	0.66	0.46	0.31-1.10	
Exchange of polyethylene	44					0.374
Yes	29	-0.428	0.65	0.65	0.31-1.48	
No	15	-0.689	0.50	0.38	0.34-1.01	

	n	Estimate	Mean* (ml)	Median (ml)	IQR (interquartile range)	p-value
BMP-7	44					0.936
Yes	7	-0.505	0.60	0.31	0.28-2.68	
No	37	-0.528	0.59	0.59	0.34-1.10	
Medication	44					0.401
Bisphosphonate	9	-0.402	0.67	0.44	0.37-1.01	
Denosumab	7	-0.446	0.64	0.46	0.32-1.77	
Bisphosphonate+denosumab	24	-0.498	0.61	0.68	0.29-1.33	
No medication	4	-0.994	0.37	0.40	0.26-0.64	
Prosthesis model	44					0.286
STAR	3	-0.959	0.38	0.48	0.15-0.79	
AES	41	-0.496	0.61	0.59	0.32-1.28	
Design of AES prosthesis	41					0.368
HA coated	10	-0.745	0.73	0.66	0.36-1.28	
Dual-coated (Ti-HA)	31	-0.421	1.03	0.46	0.31-1.52	
Location of the lesion	44					0.033
Tibia	28	-0.299	0.74	0.81	0.35-1.50	
Talus	16	-0.945	0.39	0.46	0.19-0.68	

* Statistical analyses were done for log-transformed progression values. Estimates were back-transformed to the original units.
[1] Tukey-adjusted p-value; 1 vs 2+3
[2] Tukey-adjusted p-value; 2+3 vs 4+5
[3] Tukey-adjusted p-value; 1 vs 4+5

Table 6. Pain before and after reoperation and function after reoperation. The ankles which ended-up on arthrodesis are in bold type (n = 4). (Original publication IV).

Ankle	1	2	3	4	5	6	7	8	9	10	11	12	13	14	15	16	17	18	19	20	21	22	23	24	25	26	27	28	29	30	31	32	33	34
Pain before	1	1	1	4	1	3	1	**5**	3	**5**	1	3	3	3	4	**1**	2	2	3	1	3	1	1	4	1	1	1	1	1	4	3	4	1	1
Pain after	1	1	5	2	1	3	4	**3**	5	**1**	1	4	3	4	4	**2**	1	1	3	5	3	1	1	5	1	3	1	1	3	3	1	1	1	1
Function	3	1	2	1	1	2	3	**4**	3	**4**	1	**4**	1	2	2	2	2	1	1	2	1	1	1	1	1	1	1	1	1	1	1	1	1	1

Pain: 1 = painless; 2 = starting pain; 3 = sometimes pain when loading; 4 = always pain when loading; 5 = pain at rest.
Function: 1 = notably better; 2 = little better; 3 = no change; 4 = worse (no data from 4 ankles).

during the follow-up period (Figure 8). 4 ankles ended-up in arthrodesis; 3 ankles due to malalignment and one because of infection, but none because of collapse of the components. Of the ankles that ended up in arthrodesis all except one had osteolysis on CT. Nine ankles were reoperated for a second time due to progression of osteolysis before the end of the follow-up period.

None of the demographic parameters used in this study met statistical significance as predictors of osteolytic lesions compared to those with constant bone grafting during the follow-up period. The demographic parameters were: pain ($p = 0.48$), function ($p = 0.08$), graft type ($p = 0.88$), diagnosis ($p = 0.58$), gender ($p = 0.68$), age under 50 years vs. over 50 years ($p = 0.99$), BMI under 30 vs. over 30 ($p = 0.12$), under 2 ml lesion vs. over 2 ml lesion ($p = 0.12$), exchange of polyethylene ($p = 0.76$), bone morphogenetic protein 7 (BMP-7) ($p = 0.44$), medication ($p = 0.29$), prosthesis model ($p = 0.22$), design of AES prosthesis ($p = 0.56$), and lesion location ($p = 0.17$). Two parameters were significant risk factors for progression of osteolysis during follow-up: pain ($p = 0.04$) and location of the lesion ($p = 0.03$). The demographic parameters for progression of osteolysis are shown in Table 5.

Pain before and after reoperation and postoperative function are presented in Table 6. The parameters used were modified from Kofoed's scale (Kofoed 1995). The intraobserver and interobserver reliabilities were excellent (0.89) for measuring the first postoperative volumes immediately after bone grafting. At one-year after surgery the intraobserver and the interobserver reliabilities were high, 0.79 and 0.75. At the latest measurement point during the follow-up period these reliabilities were moderate, 0.58 and 0.52, respectively.

6. DISCUSSION

6.1. TAA and periprosthetic osteolysis

6.1.1. Incidence of osteolytic lesions (Studies I, II)

The survivorship of TAA is poorer than of total hip and knee arthroplasties. Osteolysis is one of the most common mid- to long-term complication of TAA (Skyttä et al. 2010, Bonnin et al. 2011, Henricson et al. 2011, Beck et al. 2012). Osteolysis is related to many modern TAA implants, rapidly appearing and large osteolytic lesions have been typical for the AES TAA (Besse et al. 2009, Koivu et al. 2009, Kokkonen et al. 2011).

Radiographically, osteolytic lesions or radiolucent lines were detected in 48 out of 130 ankles (37%) at mean follow-up of 31.3 months (range, 3-74 months) (Study I). Major osteolytic lesions (diameter greater than 10 mm) were found in 27 ankles (Study I). There was major osteolysis on radiographs and follow-up CTs in 42 ankles (40 patients) at mean follow-up of 43.1 months (range, 14-85 months) (Study II). The number of osteolytic TAAs was high in both studies at a fairly short time interval after operation. The amount of major osteolytic lesions rose from 21% to 35% (Study I vs. Study II) when the follow-up period was prolonged with about one year. There was progression of osteolysis on radiographs in 16 ankles (33%), and here, dual-coated (Ti-HA) implants with porous coating of pure titanium and hydroxyapatite had an increase in the incidence of osteolysis that was more than 3-fold compared to implants having hydroxyapatite coating alone (Study I). In the histological samples (Study I), the amount of titanium was several-fold higher than other metals. Titanium is widely used in total joint replacements and other orthopedic hardware. It is highly biocompatible, corrosion resistant, and non-allergenic. However, it may well affect the osteolytic process (Wei et al. 2005, Purdue et al. 2007, Kaufman et al. 2008, Tamaki et al. 2008). Titanium has negative effects on osteoblasts and stimulates the release of proinflammatory mediators. Thus, titanium particles may become detached from the surface of the prosthesis components by excessive shear stresses and influence the osteolytic process. In our second study dual-coated (Ti-HA) implants were not associated with an increased incidence of osteolysis (Study II). Interestingly, male patients had a 2-fold risk for osteolysis compared to females, but not for major osteolysis (Study I).

The first major osteolytic lesion was identified as early as 14 months after TAA (Study I). Previously it has been reported that osteolytic lesions around THA appear

much later, 5 to 10 years after operation (Puri et al. 2002). An interesting question arises: Is the osteolytic process around TAA a 'different disease' than around THA or does the process of TAA osteolysis underline different components of the RANK/RANK-L/OPG pathway and in the whole biological cascade of osteolysis than the osteolytic process in THA? Osteoclasts cause bone resorption and RANK receptors occur mainly on osteoclasts. Ligand (RANK-L) binding at the receptor is the initiator for osteoclast formation and activity. RANK-L expression by macrophages, giant cells, and fibroblasts is increased in osteolytic cavities (Holding et al. 2006, Ollivere et al. 2012). Wear particles have been considered to be one of the main promoters of periprosthetic osteolysis. Wear particles are phagocytosed by macrophages, which induces proinflammatory mediators, like TNF-α. These mediators support directly osteoclast formation and indirectly by stimulating RANK/RANK-L osteoclast formation. At reoperations bacterial samples were sterile and wear debris was absent (Study I). There were large, necrotic areas in the histological samples. Similar findings with only little wear debris and large necrotic areas have been reported in periprosthetic areas around TAA in recent studies (Koivu et al. 2012, Dalat et al. 2013). A new theory claims that in the ankle the RANK/RANK-L/OPG pathway is activated by necrotic autogenous tissue rather than by polyethylene or other wear particles.

Several factors have an effect on the survivorship of TAA and probably also on osteolysis around prosthesis components in the ankle. TAA is a technically demanding procedure and the learning curve is flat (Henricson et al. 2007). Correct positioning of the prosthesis components is important, even crucial. In the standing position, large forces are directed on a small area (Vickerstaff et al. 2007). Also, the biomechanics of the ankle is complex: movement in the tibiotalar and talocalcaneal joints take space in three different planes: plantar flexion and dorsiflexion; external and internal rotation; and inversion-eversion.

Sixteen of 27 ankles with major osteolysis ended up in a reoperation (Study I). Interestingly, however, most of these patients were asymptomatic. Almost all prosthesis components were well fixed when testing during operation and the polyethylene components were visibly well preserved. Osteolysis is a continuous process, which in many cases leads finally to component failure because of critical bone stock loss. However, it can take quite a long time before bone stock breaks down. Along with the size of the osteolytic lesion, also the location of the lesion affects the decision to reoperate the ankle. Talar lesions are more difficult to handle during the reoperation and talar component subsidence is a dreadful complication. Therefore, osteolytic lesions on the talar side of the prosthesis are treated more aggressively than on the tibial side. In our hands, there was migration of the talar component in 9 ankles, but no instances of subsidence of the talar component (Study I).

6.1.2. Radiography vs. CT for detection of osteolytic lesions (Study II)

Traditionally, patients with TAA have been monitored only by radiographs. Many THA studies (Puri et al. 2002, Walde et al. 2005) have shown that radiographs underestimate periprosthetic osteolysis compared with CT. Some studies suggest that the same may be the case with regard to TAA (Hanna et al. 2007, Besse et al. 2009, Rodriguez et al. 2010, Lucas y Hernandez et al. 2014, Viste et al. 2015).

CT identified more and larger osteolytic lesions around TAAs than radiographs (Study II). Osteolytic lesions occurred in 165 zones on radiographs and in 295 zones on CT. The lesions were larger on CT than on radiographs in 9 out of 10 zones. The difference between the two imaging modalities was not significant only in zone 10. This study establishes for the first time that CT is an extremely good method to detect talar lesions. The difference between radiographs and CT in the ability to depict osteolysis was highly significant in 3 zones under the talar component (zones 5, 8 and 9) to the benefit of CT. This finding is in line with our clinical experience: the osteolytic lesions under the talar component are extremely difficult to detect on radiographs, but clinically it is most important to detect talar lesions as early as possible before dramatic subsidence of talar component occurs. As far as we know, the first study on CT and osteolysis around TAA was published by Hanna et al., who examined 17 patients (19 ankles) who had received an Agility Ankle prosthesis (Hanna et al. 2007). They included only lesions around the tibial component and in the fibula, and any possible talar lesions were not considered.

Because the osteolytic process around TAAs is continuous, CT should be performed on all patients with definite or suspected osteolysis related to TAAs on radiographs. Postoperatively it is important to detect osteolytic lesions around TAAs as soon as possible to allow appropriate decision making between reoperation and watchful waiting and CT-supported follow-up, at least of patients with asymptomatic ankles. CT shows the bone structure in greater detail around the prosthesis than radiographs and bone stock can be evaluated reliably before surgery.

There has been much discussion about the radiation dose caused by CT. As far as ankle CT is concerned this matter ought not to present any major problems. The location of an ankle joint is peripheral in the human body; and there are no radiosensitive organs in or close to the imaged region of interest. The mean effective radiation dose caused by ankle CT is 0.07 mSv, which is much less than, for example, the corresponding figure for hip CT (3.09 mSv) and even less than the figure for conventional chest radiography (0.08 mSv) (Biswas et al. 2009). The average background dose due to natural radiation exposure is 3 mSv per year (Biswas et al. 2009), which is also much higher than the dose caused by ankle CT. Thus, too much attention should not be fixed on the radiation risk, as this might unnecessarily

decrease the interest in performing ankle CTs. It can distract the attention from real medical risks rather than point to the potential benefits of CT and a timely diagnosis of a difficult-to-treat condition (osteolysis of TAA) (Balter et al. 2011). In the worst case, massive periprosthetic osteolysis could remain undetected, leading to extensive loss of bone stock and unnecessary arthrodesis, with deleterious consequences to the mobility of the patient.

6.2. CT for diagnostic evaluation of periprosthetic osteolysis after TAA (Study III)

Some previous studies have shown that radiographs give only limited information on osteolytic lesions compared to CT around TAAs (Hanna et al. 2007, [1]Kohonen et al. 2013, Viste et al. 2015). In this study we evaluated the optimal CT parameters and positioning to reduce metal artifacts when imaging TAA with CT.

All metal implants cause artifacts on CT and this distorts the image quality, which otherwise is excellent with modern CT devices. Both the material used and the orientation of the metal implant affect the amount of artifacts produced on images. Titanium causes fewer artifacts than stainless steel or cobalt-chromium (Lee et al. 2007, Stradiotti et al. 2009, Roth et al. 2012). In this study the material of the tibial and talar components were cobalt-chromium like in many other ankle prosthesis models. Despite the artifacts caused by the cobalt-chromium components, CT proved to be a reliable imaging modality of periprosthetic osteolytic lesions around TAAs. The orientation of the prosthesis seemed to be crucial; the most optimal orientation turned out to be alignment of the tibial stem parallel to the table. When the patient with TAA is lying supine on the examination table with straight knees the orientation of tibial stem is optimal, i.e., parallel to the table. The geometry of the metal implant, its cross-sectional area and size also affect artifact generation (Lee et al. 2007, Kataoka et al. 2010, Roth et al. 2012). Asymmetric hardware produces nonuniform artifacts (Roth et al. 2012). These artifacts are most prominent in the direction of the hardware's greatest cross-sectional profile (Lee et al. 2007, Roth et al. 2012).

We found that when the tibial stem was parallel to the table, the major artifacts from the tibial plate did not hide the osteolytic lesions around the tibial stem or below the talar component, i.e., in the locations where the most common lesions occur. In that position, the long axis of the tibial component was perpendicular to the plane of the gantry. With higher angles, i.e., when the tibial stem was at an angle of 25°, 45°, and 90° to the table, there were significant differences between the volume measurements by CT compared to real volumes because of pronounced image artifacts. The orientation of the artifact lines was unfavorable at higher

angles when considering such periprosthetic lytic lesions. Also, the sum effect of the artifacts from the plate and stem probably played a role in impairing image quality. In most of these cases, the presence of artifacts led to an underestimation of the volume of the drilled defect. When the tibial stem was at a 45° or a 90° angle to the table, smaller defects (volumes of 0.55 ml and 0.5 ml) around the tibial and the talar components could not be detected by CT, because of major artifacts at every studied kVp.

A high tube voltage (140 kVp) is usually recommended for imaging of sites containing metal hardware by CT for minimizing artifacts (Puri et al. 2002, Douglas-Akinwande et al. 2006, Hanna et al. 2007). Higher kilovoltage reduces noise, but diminishes image contrast and increases radiation dose. Lee et al. studied the effects of a titanium alloy screw and a stainless-steel screw placed in a pig femur. When comparing the axial CT images obtained through the screws with two different kilovolt peaks, 140 kVp and 80 kVp, and with the other parameters fixed, the higher peak voltage yielded fewer artifacts (Lee et al. 2007). In another study 140 kVp tube voltage instead of 120 kVp did not improve imaging of metallic components (Haramati et al. 1994). However, the number of imaged patients was only three – two with a THA (titanium and cobalt-chromium) and one with a pelvis reconstruction with stainless-steel plates. In our study there were no significant differences between the three different tube voltages (100, 120, and 140 kVp) as far as volume measurements are concerned (Study III). However, when scanning at a 90° angle at 100 kVp and 120 kVp, the larger defect (volume 1.5 ml) around the talar component could not be detected at all on images because of artifacts. When scanning at 140 kVp (with a 90° angle) the larger defect in talus was barely visible. According to this study (Study III), 100 kVp is sufficient for evaluation of periprosthetic lesions around TAAs, provided that the orientation of the ankle prosthesis is optimal.

Lowering the pitch settings has been shown to diminish artifacts, but it increases the radiation dose (Lee et al. 2007, Ohashi and El-Khoury 2009, Buckwalter et al. 2011). A lower pitch setting increases the likelihood that adequate data will be gathered (Stradiotti et al. 2009). We did not find significant differences in the volume measurements of the periprosthetic lesions when we used different pitches (1 and 1.2) at 120 kVp (Study III).

The computed tomography dose volume index ($CTDI_{vol}$) values in this study were over twofold when kVp increased from 100 to 140 (Table 7). $CTDI_{vol}$ does not, however, represent patient dose; rather, it describes the radiation output of a CT system. In this study tube current modulation was used. Higher mAs values result in more photons being detected. Increasing the tube current (mAs) reduces noise,

Table 7. Imaging parameters and data in different protocols and positions. There were 16 different imaging protocols. Angle refers to the alignment of tibial stem to table. (Original publication III).

Angle (degrees)	kVp	Pitch	CTDI$_{vol}$ (CT dose volume index, mGy)	Distance imaged (cm)	mAs min	mAs max	Cumulative mAs	No of detected defects
0	100	1.2	4.81	16.8	85	115	6023	4
0	120	1.2	8.28	16.8	83	112	5962	4
0	120	1.0	8.27	16.8	85	113	6070	4
0	140	1.2	12.9	16.8	77	112	5919	4
25	100	1.2	4.88	16.8	89	116	6032	4
25	120	1.2	8.28	16.8	90	112	5972	4
25	120	1.0	8.27	16.8	94	113	6037	4
25	140	1.2	12.9	16.8	92	112	5957	4
45	100	1.2	4.81	18.9	87	114	6748	2
45	120	1.2	8.28	18.9	86	116	6740	2
45	120	1.0	8.16	19.2	90	116	6789	2
45	140	1.2	12.75	19.9	88	112	6617	2
90	100	1.2	4.29	12.3	67	115	3909	1
90	120	1.2	7.39	12.3	65	113	3830	1
90	120	1.0	7.51	12.6	71	111	4107	1
90	140	1.2	12.2	12.6	72	111	4239	2

but increases the radiation dose (Kataoka et al. 2010, Roth et al. 2012). When we scanned the ankle prosthesis at a 90° angle, the lowest cumulative mAs values were measured (Table 7), probably due to the fact that the imaged distance was shortest in that orientation. The differences in imaging distances and cumulative mAs values were small in the other orientations.

After this sub-study, iterative reconstruction has been brought widely into clinical practice, one of the fruits of higher computational power of modern workstations (Boudabbous et al. 2015). Nowadays all major vendors have iterative reconstruction algorithms for clinical use (Willemink et al. 2013). Also, dual-energy CT is used at an increasing rate in clinical practice (Coupal et al. 2014, Filograna et al. 2016). Both of these methods reduce metal artifacts without need to raise the radiation dose. Iterative reconstruction or DECT were not evaluated in this sub-study.

6.3. Follow-up after bone grafting of osteolytic lesions around TAA (Study IV)

68% of the osteolytic lesions progressed radiologically during follow-up. Osteolysis progressed slightly less (63%) in ankles with an excellent postoperative grafting status (no residual lesion immediately after reoperation). Thus, a good postoperative grafting status does not seem to protect against progression of osteolysis. 58% of

the osteolytic lesions continued to progress already during the first follow-up year, and once this had started, it continued in 74% in the second follow-up period (one year after reoperation vs. latest follow-up). Periprosthetic osteolysis is probably a continuous process which often leads to component failure. Our result with excellent radiographic survivorship in almost one third (28%) of bone-grafted lesions is at least promising. The final goal of bone grafting is to avoid arthrodesis or at least to prolong the time before arthrodesis becomes mandatory. In our study only four ankles of 34 ended up in arthrodesis. Bone grafting may be considered as a satisfactory method to avoid arthrodesis, something that took place in 88% of the ankles (Study IV). Upcoming studies will describe the course of bone-grafted lesions and the behavior of the graft and establish if some of the osteolytic lesions stabilize later on after bone grafting.

There are no guidelines for the surgical treatment of periprosthetic osteolytic lesions around TAA. The general goal is to restore bone stock. Other principles are to remove the source of wear particles, debris itself, and any apparent necrotic tissue (Stulberg and Della Valle 2008, Dalat et al. 2013, Koivu et al. 2015). There are only a few reports in the literature on TAA survivorship after bone grafting of periprosthetic osteolytic lesions. In none of these studies was systematic CT follow-up after reoperation carried out. In a study of Yoon et al. there was no radiographic progression of bone-grafted lesions among 8 patients with TAA (Yoon et al. 2014). The follow-up period was short, only 15.3 months. In another retrospective evaluation of 31 patients, grafting of osteolytic lesions without revision of prosthesis components was considered an effective and safe means for treating periprosthetic osteolysis around TAA (Gross et al. 2016). During a median follow-up of 12.2 months 4 patients ended up in arthrodesis or component revision. Mann et al. recommended immediate bone grafting if osteolytic lesions were found in multiple areas around the TAA, as well as in cases with progression of lesions (Mann et al. 2011). Our results also favor bone grafting of osteolytic lesions around TAA.

There are also contrary conclusions. Besse et al. followed 14 patients with AES TAAs after treatment of periprosthetic osteolytic lesions (Besse et al. 2013). 4 types of filling material were used: autografts in 7 patients, corticocancellous-calcium phosphate graft in one patient, calcium phosphate cement grafts in 4 patients, and polymethylmethacrylate cement grafts in 2 patients. 4 patients ended up in arthrodesis. Of the remaining 10 patients, 6 developed recurrent cysts and 2 had lucencies at the bone-cement interphase. The follow-up period of 2 patients was too short for radiologic evaluation. Based on the high frequency of arthrodesis and recurrent cysts the authors no longer recommended grafting of osteolytic lesions around TAA. They suggested annual radiological evaluation, also by CT if the osteolytic lesions kept on enlarging, or the ankle was painful. They considered CT

to have a specific role for timing of implant removal and reconstruction-arthrodesis before the talar component collapses.

Both allograft and autograft material was used in our study, and in one operation both (Study IV). Neither of them proved to be superior in preventing the appearance or progression of osteolytic lesions. All in all, however, the number of lesions filled with autograft was low. The polyethylene insert is often exchanged in connection with the reoperation, although the exact role of polyethylene in the pathogenesis of osteolysis is not precisely known. In this study the polyethylene component was changed in most ankles (71%). Changing the polyethylene insert did not prevent significantly the appearance or progression of osteolysis.

None of the demographic parameters studied turned out to be a significant risk factor for appearing of osteolysis in the bone grafted areas. However, progression of osteolysis was significant of lesions located in tibia and of painless lesions. For unknown reasons there was more progression of tibial lesions than talar lesions (p = 0.03). Interestingly, there was more progression in osteolytic lesions in painless ankles compared to ankles with pain (p = 0.04). One explanation for this could be that patients with painless ankles use their ankles more and maybe in more extreme postures exposing the prosthesis components for a high level of burden. In our previous study (Koivu et al. 2009), the risk for osteolysis was higher with dual-coated (Ti-HA) AES implants than with HA coated implants, also for male patients compared to females. The coating of the prosthesis components or the gender of the patient were not significantly associated with survivorship of the bone-grafted lesions in this study (Study IV).

Clinically, the pain experienced by the patients was not influenced by surgery in 17 patients; 15 ankles were totally painless after reoperation, 11 ankles had start-up pain or occasional pain when loading, and 8 ankles were constantly painful on loading and at rest (Study IV). Subjective function of the ankle joint was notably better in 19 ankles after reoperation, little better in 6 ankles, unchanged in 3 ankles and worse only in 2 ankles (no data for 4 ankles). The result that at least 25 ankles were functionally better after reoperation is fairly good. Comparison of radiological and clinical survivorship was difficult because many ankles had simultaneously lesions with excellent radiological survivorship and lesions with progressive osteolysis. Both intraobserver and interobserver reliabilities were excellent at the first measurement point after reoperation and good at the 1-year postoperative control. At the latest measurement point reliability was only moderate. One possible reason for that may be that immediately after reoperation there were more zero values (= no residual) than at the time of the other measurements. When measuring the volumes of the osteolytic cavities around prosthesis components there was good

agreement of zero values. When there was a recurrence or residual lesion on CT, it was not always easy to define with certainty the exact borders of the lesion because of complex morphology of the lesion and some metal artifacts which distorted the image quality near the prosthetic components.

A strength of this study is the large number of ankles (n = 34) including 65 bone-grafted lesions which we followed by CT for an average of 3.8 years (range, 2.0-6.2 years). A limitation of this study is its retrospective design and heterogeneous use of the medication. Due to this variability it was not possible to analyze the effect of medication on the appearance or progression of osteolysis related to grafted lesions. So far, no effective medical treatment has been reported in the literature to treat periprosthetic osteolysis. There are some candidate drugs which might be useful in the treatment of peri-implant osteolysis based on their success in other indications, e.g., bisphosphonates and denosumab (Purdue et al. 2006, Schwarz 2008). There was no significant difference between the ankles augmented with a bone morphogenetic protein-7 (BMP-7) product compared to those with plain bone grafting in survivorship of the grafted lesions in our study (Study IV). However, BMP-7 was used only in 5 operations. According to a study by White et al., BMP-7 is useful for the treatment of fractures, non-unions, and in spinal fusion (White et al. 2007). A limitation is also that altogether 5 orthopedic surgeons performed the reoperations, although two of them did participate in 88% of the reoperations. Only 3 STAR TAAs were included in this study, all the other were AES TAAs. The AES TAA has been withdrawn from the market due to its relation with early-onset osteolysis. However, osteolysis is a common problem related to many modern total ankle implants, and the AES implant serves as a good model for studying osteolysis.

It is still unclear why some patients with TAA develop peri-implant osteolysis and others do not. The most favorable treatment of TAA-associated periprosthetic osteolysis is still not known. In this study, there was radiological progression of osteolysis in 68% of the bone-grafted lesions around the TAA, and four ankles ended-up in arthrodesis during follow-up (Study IV). However, in 18 bone-grafted lesions (28%) radiological survivorship was excellent. We consider that grafting is still the treatment of choice of osteolytic lesions for some TAA patients with osteolysis, but challenges are posed by the selection of patients and the timing of the reoperation.

6.4. Limitations of the study

We studied mainly AES TAAs and only 3 STAR TAAs were included in Study IV. The AES TAA is no longer commercially available, since AES has given rise to alarming reports of osteolytic lesions (Besse et al. 2009, Koivu et al. 2009). However, there

are several prostheses in the market with similar configurations and materials as the AES.

In Study I the systematic evaluation of periprosthetic osteolysis was done only by radiographs, although we knew that CT is probably a more accurate method for detecting osteolytic lesions around TAA. The radiographs were evaluated by two independent observers. The final conclusions were drawn in consensus, so interobserver reliability evaluation was not performed.

In Study II we had no pathological or surgical confirmation of the exact size of the osteolytic lesions around the AES TAAs. Nor did we have preoperative CT images; it is possible that some of the lesions were degenerative cysts or geodes rather than osteolytic lesions. To analyze both radiographs and CT images we used the protocol of Besse et al., which has been designed for radiographs (Besse et al. 2009). Because the purpose of this study was to compare radiographs and CT, we chose the same protocol for both imaging modalities, although surface area measurements or volumetric measurements on CT images could have been possible and probably more accurate. Interobserver reliability evaluation was not done in this study, instead consensus conclusions of two independent observers were used. There was a high number of osteolytic lesions both by radiography (n = 165) and especially by CT (n = 295). However, the real number of osteolytic lesions was not so big, because osteolytic change in 2 or several different zones could represent the same lesion. Based on this study it was difficult to report the exact number of osteolytic lesions. The maximum time interval between CT and preceding radiography was 23 months (mean, 5.6 months) and it is thus possible that some of the osteolytic lesions had truly increased in size between the two studies. Finally, we did not know the patients' clinical outcomes, since only imaging methods were compared.

In the experimental study (Study III), we examined only one sample (one porcine knee joint) with the AES prosthesis implanted in it, and obviously we could not make any statistical comparisons or judge the effect of interindividual variation. Only one radiologist measured the size of the defects on the CT images. It was difficult to make this radiologist blinded with regard to image settings. Using the workstation available, the radiologist could easily see the orientation of the prosthesis components used at the time of imaging and she also knew on beforehand the number of defects around the prosthesis components. Newer MAR image reconstruction algorithms such as iterative reconstruction were not evaluated in this study.

In Study IV, medication to treat osteolysis and the use of BMP-7 in connection with the reoperation were heterogeneous because of retrospective nature of the

study. Neither of these parameters was a significant risk factor for appearing or progression of osteolysis. Because of the great variability of these parameters, it is not feasible to draw any far-reaching conclusions on the basis of the results. A further limitation is that altogether 5 orthopedic surgeons were involved in doing the reoperations, although two of them did participate in 88% of the reoperations.

6.5.   Future considerations

We found that osteolysis is common around TAAs. It would be interesting to screen all our TAA patients by CT to establish the real number of osteolytic lesions. It is crucial to remember that patients, even asymptomatic, may have progressing osteolysis despite no visible osteolytic lesions on radiographs.

Newer MAR image reconstruction algorithms, such as iterative reconstruction, were not used in this study. During the recent years iterative reconstruction has been used more often in clinical practice, because of increased computational power of workstations. Iterative reconstruction methods and TAA should be studied to identify the ability of the new reconstruction methods of the CT-technology to reduce metal artifacts around prosthesis components. DECT is a novel technique to reduce artifacts caused by metallic implants. DECT was not either evaluated in this study. It would be interesting to use DECT to establish the optimal monochromatic image parameters for diminishing metal artifacts around TAA.

At present, metal artifacts can be adequately handled in MRI with MARS. It would be extremely interesting to study osteolytic lesions around TAAs with MRI, which apparently has not been done so far.

Osteolysis around TAA remains unsolved and the optimal total ankle prosthesis awaits its inventor. Despite osteolysis, there is progressive interest in TAA, because long-term survivorship of modern prosthesis models is acceptable today and will hopefully improve in the future. Nevertheless, as long as periprosthetic osteolysis contributes so markedly to TAA complications, accurate and accessible imaging modalities are needed. Studies with CT and MRI are needed to further improve imaging parameters and sequences in an effort to reduce metal artifacts around TAAs.

7. CONCLUSIONS

The following conclusions may be drawn from the studies presented in this thesis.

1. Ankle radiographs showed that early-onset periprosthetic osteolysis is common (37%) around AES total ankle arthroplasties. The risk factors for osteolysis are the use of dual-coated implants (Ti-HA) and male gender. At reoperations there was no bacterial growth in the samples from osteolytic cavities and surrounding structures, but the amount of titanium was high in the samples.

2. CT reveals more and larger osteolytic lesions than radiographs around TAAs. The difference was statistically significant ($p < 0.05$) in 9 out of 10 zones around the total ankle prosthesis and highly significant ($p < 0.0001$) in three zones around the talar component.

3. CT is a reliable imaging method for evaluation of the bone structure around ankle prostheses when acquisition parameters and especially the orientation of the prosthesis are optimized. Supposing that the ankle is in optimal orientation, i.e. the tibial stem alignment parallel to the table, 100 kVp is adequate to evaluate periprosthetic bone structure.

4. Radiological progression of osteolysis was high (68%) after bone grafting of periprosthetic osteolytic lesions around total ankle arthroplasties. In 28% of grafted lesions the radiological survivorship was excellent during a mean follow-up of 3.8 years (range, 2.0-6.2 years).

8.   ACKNOWLEDGEMENTS

a professional role model for me, and I have to say you could not be any better. And Pirkko, I want to thank you for all those wise words you have said to me concerning radiology and life in general. Teemu Paavilainen and Jari Karhu, for keeping up a joyful and relaxed atmosphere at work; your funny stories have saved my day so many times. Professor Peter Dean, for being the first person who raised my interest in the amazing world of radiology.

The outstanding group of ladies, or ´girls´, as we call each other, for sharing the ups and downs in life. I am really honored to have friends like you. Anu Ukkonen, Satu Antila, Kati Sven, Kati Wink, Johanna Ekman and Terhi Tamminen - my dear friends at least for 30 years, we have spent so many happy and hilarious moments together. Also, my closest friends from medical school: Laura Hakkala, Katri Louhi and Laura Ravanti. Without you lectures and studying in general would have been much more boring. I will always remember our ´ex tempore trip´ to the parties at the Polytechnic Department of Tampere, and I will certainly remember the after-party lecture next morning at the medical school in Turku.

Liisa and Reijo Halme, Tiina and Olli Alikärri and their children, for friendship, support and all the time we have spent together.

My dear younger brothers, Keijo and Ilmari and their families, for sharing so many precious, joyful and happy moments. I am really fortunate having so many wonderful and beloved people in my life. My dear parents, Tuula and Martti, for their never-ending love and encouragement. I have always felt that they have supported me whatever I have decided to do. Mum, I really admire your enthusiasm and endless interest in different things in life, and also the ability to be up to date although retired. Your practical help in numerous situations has been crucial. And dad, you really are the kindest man I have ever known – your tireless interest towards my projects and ideas has strengthened me.

Above all, dear Perttu, for sharing almost all of your adult life with me. I am happy we have got through so far. I love You to the moon and back.

Turku, December 2016

Ia Kohonen

9. REFERENCES

Anderson T, Montgomery F, Carlsson A. Uncemented STAR total ankle prostheses. Three to eight-year follow-up of fifty-one consecutive ankles. J Bone Joint Surg Am 2003;85-A(7):1321-1329.

Archibeck MJ, Jacobs JJ, Roebuck KA, Glant TT. The basic science of periprosthetic osteolysis. Instr Course Lect 2001;50:185-195.

Atkinson HD, Ranawat VS, Oakeshott RD. Granuloma debridement and the use of an injectable calcium phosphate bone cement in the treatment of osteolysis in an uncemented total knee replacement. J Orthop Surg and Res 2010;5(29):1-6.

Balter S, Zanzonico P, Reiss GR, Moses JW. Radiation is not the only risk. AJR Am J Roentgenol 2011;196(4):762-767.

Bamberg F, Dierks A, Nikolaou K, Reiser MF, Becker CR, Johnson TR. Metal artifact reduction by dual energy computed tomography using monoenergetic extrapolation. Eur Radiol 2011;21(7):1424-1429.

Barrett JF, Keat N. Artifacts in CT: recognition and avoidance. Radiographics 2004;24(6):1679-1691.

Beck RT, Illingworth KD, Saleh KJ. Review of periprosthetic osteolysis in total joint arthroplasty: an emphasis on host factors and future directions. J Orthop Res 2012;30(4):541-546.

Besse JL, Brito N, Lienhart C. Clinical evaluation and radiographic assessment of bone lysis of the AES total ankle replacement. Foot Ankle Int 2009;30(10):964-975.

Besse JL, Lienhart C, Fessy MH. Outcomes following cyst curettage and bone grafting for the management of periprosthetic cystic evolution after AES total ankle replacement. Clin Podiatr Med Surg 2013;30(2):157-170.

Bestic JM, Peterson JJ, DeOrio JK, Bancroft LW, Berquist TH, Kransdorf MJ. Postoperative evaluation of the total ankle arthroplasty. AJR Am J Roentgenol 2008;190(4):1112-1123.

Biswas D, Bible JE, Bohan M, Simpson AK, Whang PG, Grauer JN. Radiation exposure from musculoskeletal computerized tomographic scans. J Bone Joint Surg Am 2009;91(8):1882-1889.

Bolton-Maggs BG, Sudlow RA, Freeman MA. Total ankle arthroplasty. A long-term review of the London Hospital experience. J Bone Joint Surg Br 1985;67(5):785-790.

Bonnin M, Gaudot F, Laurent JR, Ellis S, Colombier JA, Judet T. The Salto total ankle arthroplasty: survivorship and analysis of failures at 7 to 11 years. Clin Orthop Relat Res 2011;469(1):225-236.

Boudabbous S, Arditi D, Paulin E, Syrogiannopoulou A, Becker C, Montet X. Model-Based Iterative Reconstruction (MBIR) for the reduction of metal artifacts on CT. AJR Am J Roentgenol 2015;205(2):380-385.

Buckwalter KA, Lin C, Ford JM. Managing postoperative artifacts on computed tomography and magnetic resonance imaging. Semin Musculoskelet Radiol 2011;15(4):309-319.

Coester LM, Saltzman CL, Leupold J, Pontarelli W. Long-term results following ankle arthrodesis for post-traumatic arthritis. J Bone Joint Surg Am 2001;83-A(2):219-228.

Costello JE, Cecava ND, Tucker JE, Bau JL. CT radiation dose: current controversies and dose reduction strategies. AJR Am J Roentgenol 2013;201(6):1283-1290.

Cottrino S, Fabrègue D, Cowie AP, Besse J-L, Tadier S, Gremillard L, Hartmann DJ. Wear study of total ankle replacement explants by microstructural analysis. J Mech Behav Biomed Mater 2016;61(I-II):1-11.

Coupal TM, Mallinson PI, McLaughlin P, Nicolaou S, Munk PL, Ouellette H. Peering through the glare: using dual-energy CT to overcome the problem of metal artefacts in bone radiology. Skeletal Radiol 2014;43(5):567-575.

Dalat F, Barnoud R, Fessy MH, Besse JL, French Association of Foot Surgery AFCP. Histologic study of periprosthetic osteolytic lesions after AES total ankle replacement. A 22 case series. Orthop Traumatol Surg Res 2013;99(6 Suppl):S285-295.

Daniels TR, Younger AS, Penner M, Wing K, Dryden PJ, Wong H, et al. Intermediate-term results of total ankle replacement and ankle arthrodesis: a COFAS multicenter study. J Bone Joint Surg Am 2014;96(2):135-142.

Demetracopoulos CA, Adams SB,Jr, Queen RM, DeOrio JK, Nunley JA,2nd, Easley ME. Effect of age on outcomes in total ankle arthroplasty. Foot Ankle Int 2015;36(8):871-880.

DiDomenico LA, Cross D. Revision of failed ankle implants. Clin Podiatr Med Surg 2012;29(4):571-584.

Doets HC, Brand R, Nelissen RG. Total ankle arthroplasty in inflammatory joint disease with use of two mobile-bearing designs. J Bone Joint Surg Am 2006;88(6):1272-1284.

Dougeni E, Faulkner K, Panayiotakis G. A review of patient dose and optimisation methods in adult and paediatric CT scanning. Eur J Radiol 2012;81(4):e665-683.

Douglas-Akinwande AC, Buckwalter KA, Rydberg J, Rankin JL, Choplin RH. Multichannel CT: evaluating the spine in postoperative patients with orthopedic hardware. Radiographics 2006;26 Suppl 1:S97-110.

Easley ME, Adams SB,Jr, Hembree WC, DeOrio JK. Results of total ankle arthroplasty. J Bone Joint Surg Am 2011;93(15):1455-1468.

Ellington JK, Gupta S, Myerson MS. Management of failures of total ankle replacement with the agility total ankle arthroplasty. J Bone Joint Surg Am 2013;95(23):2112-2118.

Filograna L, Magarelli N, Leone A, Guggenberger R, Winklhofer S, Thali MJ, et al. Value of monoenergetic dual-energy CT (DECT) for artefact reduction from metallic orthopedic implants in post-mortem studies. Skeletal Radiol 2015;44(9):1287-1294.

Filograna L, Magarelli N, Leone A, de Waure C, Calabro GE, Finkenstaedt T, et al. Performances of low-dose dual-energy CT in reducing artifacts from implanted metallic orthopedic devices. Skeletal Radiol 2016;45(7):937-947.

Gaden MT, Ollivere BJ. Periprosthetic aseptic osteolysis in total ankle replacement: cause and management. Clin Podiatr Med Surg 2013;30(2):145-155.

Gougoulias NE, Khanna A, Maffulli N. History and evolution in total ankle arthroplasty. Br Med Bull 2009;89:111-151.

Gougoulias N, Khanna A, Maffulli N. How successful are current ankle replacements?: a systematic review of the literature. Clin Orthop Relat Res 2010;468(1):199-208.

Gougoulias N, Maffulli N. History of total ankle replacement. Clin Podiatr Med Surg 2013;30(1):1-20.

Gross CE, Huh J, Green C, Shah S, DeOrio JK, Easley M, et al. Outcomes of bone grafting of bone cysts after total ankle arthroplasty. Foot Ankle Int 2016;37(2):157-164.

Gupta S, Ellington JK, Myerson MS. Management of specific complications after revision total ankle replacement. Semin Arthroplasty 2010;21(4):310-319.

Göthlin JH, Geijer M. The utility of digital linear tomosynthesis imaging of total hip joint arthroplasty with suspicion of loosening: a prospective study in 40 patients. BioMed Res Int vol. 2013, 6 pages.

Haddad SL, Coetzee JC, Estok R, Fahrbach K, Banel D, Nalysnyk L. Intermediate and long-term outcomes of total ankle arthroplasty and ankle arthrodesis. A systematic review of the literature. J Bone Joint Surg Am 2007;89(9):1899-1905.

Hanna RS, Haddad SL, Lazarus ML. Evaluation of periprosthetic lucency after total ankle arthroplasty: helical CT versus conventional radiography. Foot Ankle Int 2007;28(8):921-926.

Haramati N, Staron RB, Mazel-Sperling K, Freeman K, Nickoloff EL, Barax C, et al. CT scans through metal scanning technique versus hardware composition. Comput Med Imaging Graph 1994;18(6):429-434.

Harris WH, Schiller AL, Scholler JM, Freiberg RA, Scott R. Extensive localized bone resorption in the femur following total hip replacement. J Bone Joint Surg Am 1976;58(5):612-618.

Henricson A, Skoog A, Carlsson A. The Swedish Ankle Arthroplasty Register: an analysis of 531 arthroplasties between 1993 and 2005. Acta Orthop 2007;78(5):569-574.

Henricson A, Nilsson JA, Carlsson A. 10-year survival of total ankle arthroplasties: a report on 780 cases from the Swedish Ankle Register. Acta Orthop 2011;82(6):655-659.

Holding CA, Findlay DM, Stamenkov R, Neale SD, Lucas H, Dharmapatni ASSK, et al. The correlation of RANK, RANKL and TNFα expression with bone loss volume and polyethylene wear debris around hip implants. Biomaterials 2006;27(30):5212-5219.

Hounsfield GN. Computerized transverse axial scanning (tomography). 1. Description of system. Br J Radiol 1973;46(552):1016-1022.

Hozack WJ, Mesa JJ, Carey C, Rothman RH. Relationship between polyethylene wear, pelvic osteolysis, and clinical symptomatology in patients with cementless acetabular components. A framework for decision making. J Arthroplasty 1996;11(7):769-772.

Hsu AR, Haddad SL, Myerson MS. Evaluation and management of the painful total ankle arthroplasty. J Am Acad Orthop Surg 2015;23(5):272-282.

Jonck JH, Myerson MS. Revision total ankle replacement. Foot Ankle Clin 2012;17(4):687-706.

Kalender WA. X-ray computed tomography. Phys Med Biol 2006;51(13):R29-43.

Kataoka ML, Hochman MG, Rodriguez EK, Lin PJ, Kubo S, Raptopolous VD. A review of factors that affect artifact from metallic hardware on multi-row detector computed tomography. Curr Probl Diagn Radiol 2010;39(4):125-136.

Kaufman AM, Alabre CI, Rubash HE, Shanbhag AS. Human macrophage response to UHMWPE, TiAlV, CoCr, and alumina particles: analysis of multiple cytokines using protein arrays. J Biomed Mater Res A 2008;84(2):464-474.

Knecht SI, Estin M, Callaghan JJ, Zimmerman MB, Alliman KJ, Alvine FG, et al. The Agility total ankle arthroplasty. Seven to sixteen-year follow-up. J Bone Joint Surg Am 2004;86-A(6):1161-1171.

Kofoed H. Cylindrical cemented ankle arthroplasty: a prospective series with long-term follow-up. Foot Ankle Int 1995;16(8):474-479.

Kofoed H, Lundberg-Jensen A. Ankle arthroplasty in patients younger and older than 50 years: a prospective series with long-term follow-up. Foot Ankle Int 1999;20(8):501-506.

[1]Kohonen I, Koivu H, Pudas T, Tiusanen H, Vahlberg T, Mattila K. Does computed tomography add information on radiographic analysis in detecting periprosthetic osteolysis after total ankle arthroplasty? Foot Ankle Int 2013;34(2):180-188.

[2]Kohonen I, Koivu H, Vahlberg T, Larjava H, Mattila K. Total ankle arthroplasty: optimizing computed tomography imaging protocol. Skeletal Radiol 2013;42(11):1507-1513.

Koivu H, Kohonen I, Sipola E, Alanen K, Vahlberg T, Tiusanen H. Severe periprosthetic osteolytic lesions after the Ankle Evolutive System total ankle replacement. J Bone Joint Surg Br 2009;91(7):907-914.

Koivu H, Mackiewicz Z, Takakubo Y, Trokovic N, Pajarinen J, Konttinen YT. RANKL in the osteolysis of AES total ankle replacement implants. Bone 2012;51(3):546-552.

Koivu H, Takakubo Y, Mackiewicz Z, Al-Samadi A, Soininen A, Peled N, et al. Autoinflammation around AES total ankle replacement implants. Foot Ankle Int 2015;36(12):1455-1462.

Kokkonen A, Ikavalko M, Tiihonen R, Kautiainen H, Belt EA. High rate of osteolytic lesions in medium-term followup after the AES total ankle replacement. Foot Ankle Int 2011;32(2):168-175.

Kotnis R, Pasapula C, Anwar F, Cooke PH, Sharp RJ. The management of failed ankle replacement. J Bone Joint Surg Br 2006;88(8):1039-1047.

Krause FG, Windolf M, Bora B, Penner MJ, Wing KJ, Younger AS. Impact of complications in total ankle replacement and ankle arthrodesis analyzed with a validated outcome measurement. J Bone Joint Surg Am 2011;93(9):830-839.

Lavernia CJ. Cost-effectiveness of early surgical intervention in silent osteolysis. J Arthroplasty 1998;13(3):277-279.

Lee MJ, Kim S, Lee SA, Song HT, Huh YM, Kim DH, et al. Overcoming artifacts from metallic orthopedic implants at high-field-strength MR imaging and multi-detector CT. Radiographics 2007;27(3):791-803.

Liu PT, Pavlicek WP, Peter MB, Spangehl MJ, Roberts CC, Paden RG. Metal artifact reduction image reconstruction algorithm for CT of implanted metal orthopedic devices: a work in progress. Skeletal Radiol 2009;38(8):797-802.

Looney RJ, Boyd A, Totterman S, Seo GS, Tamez-Pena J, Campbell D, et al. Volumetric computerized tomography as a measurement of periprosthetic acetabular osteolysis and its correlation with wear. Arthritis Res 2002;4(1):59-63.

Lord G, Marotte JH. Total ankle replacement (author's transl). Rev Chir Orthop Reparatrice Appar Mot 1980;66(8):527-530.

Lucas y Hernandez J, Laffenetre O, Toullec E, Darcel V, Chauveaux D. AKILE total ankle arthroplasty: clinical and CT scan analysis of periprosthetic cysts. Orthop Traumatol Surg Res 2014;100(8):907-915.

Malan DF, Botha CP, Kraaij G, Joemai RM, van der Heide HJ, Nelissen RG, et al. Measuring femoral lesions despite CT metal artefacts: a cadaveric study. Skeletal Radiol 2012;41(5):547-555.

Mann JA, Mann RA, Horton E. STAR ankle: long-term results. Foot Ankle Int 2011;32(5):S473-484.

McCollough CH, Leng S, Yu L, Cody DD, Boone JM, McNitt-Gray MF. CT dose index and patient dose: they are not the same thing. Radiology 2011;259(2):311-316.

McNitt-Gray MF. AAPM/RSNA Physics tutorial for residents: topics in CT. Radiation dose in CT. Radiographics 2002;22(6):1541-1553.

Mercer J, Penner M, Wing K, Younger Alastair SE. Inconsistency in the reporting of adverse events in total ankle arthroplasty: a systematic review of the literature. Foot Ankle Int 2016;37(2):127-136.

Mettler FA,Jr, Bhargavan M, Faulkner K, Gilley DB, Gray JE, Ibbott GS, et al. Radiologic and nuclear medicine studies in the United States and worldwide: frequency, radiation dose, and comparison with other radiation sources--1950-2007. Radiology 2009;253(2):520-531.

Morsbach F, Bickelhaupt S, Wanner GA, Krauss A, Schmidt B, Alkadhi H. Reduction of metal artifacts from hip prostheses on CT images of the pelvis: value of iterative reconstructions. Radiology 2013;268(1):237-244.

Myerson MS, Won HY. Primary and revision total ankle replacement using custom-designed prostheses. Foot Ankle Clin 2008;13(3):521-538.

Nicolaou S, Liang T, Murphy DT, Korzan JR, Ouellette H, Munk P. Dual-energy CT: a promising new technique for assessment of the musculoskeletal system. AJR Am J Roentgenol 2012;199(5 Suppl):S78-86.

Nieuwe Weme RA, van Solinge G, N Doornberg J, Sierevelt I, Haverkamp D, Doets HC. Total ankle replacement for posttraumatic arthritis. Similar outcome in postfracture and instability arthritis: a comparison of 90 ankles. Acta Orthop 2015;86(4):401-406.

No authors listed. NIOSH Manual of Analytical Methods (NMAM). http://www.cdc.gov/niosh/nmam/.

Ohashi K, El-Khoury GY. Musculoskeletal CT: recent advances and current clinical applications. Radiol Clin North Am 2009;47(3):387-409.

Ollivere B, Wimhurst JA, Clark IM, Donell ST. Current concepts in osteolysis. J Bone Joint Surg Br 2012;94(1):10-15.

Park JS, Ryu KN, Hong HP, Park YK, Chun YS, Yoo MC. Focal osteolysis in total hip replacement: CT findings. Skeletal Radiol 2004;33(11):632-640.

Park JS, Mroczek KJ. Total ankle arthroplasty. Bull NYU Hosp Jt Dis 2011;69(1):27-35.

Potter HG, Foo LF, Nestor BJ. What is the role of magnetic resonance imaging in the evaluation of total hip arthroplasty? HSS J 2005;1(1):89-93.

Potter HG, Foo LF. Magnetic resonance imaging of joint arthroplasty. Orthop Clin North Am 2006;37(3):361-373.

Purdue PE, Koulouvaris P, Nestor BJ, Sculco TP. The central role of wear debris in periprosthetic osteolysis. HSS J 2006;2(2):102-113.

Purdue PE, Koulouvaris P, Potter HG, Nestor BJ, Sculco TP. The cellular and molecular biology of periprosthetic osteolysis. Clin Orthop Relat Res 2007;454:251-261.

Puri L, Wixson RL, Stern SH, Kohli J, Hendrix RW, Stulberg SD. Use of helical computed tomography for the assessment of acetabular osteolysis after total hip arthroplasty. J Bone Joint Surg Am 2002;84-A(4):609-614.

Rodriguez D, Bevernage BD, Maldague P, Deleu PA, Tribak K, Leemrijse T. Medium term follow-up of the AES ankle prosthesis: High rate of asymptomatic osteolysis. Foot Ankle Surg 2010;16(2):54-60.

Roth TD, Maertz NA, Parr JA, Buckwalter KA, Choplin RH. CT of the hip prosthesis: appearance of components, fixation, and complications. Radiographics 2012;32(4):1089-1107.

Sandgren B, Skorpil M, Nowik P, Olivercrona H, Crafoord J, Weidenhielm L, et al. Assessment of wear and periacetabular osteolysis using dual energy computed tomography on a pig cadaver to identify the lowest acceptable radiation dose. Bone Joint Res 2016;5(7):307-313.

Schindera ST, Odedra D, Raza SA, Kim TK, Jang HJ, Szucs-Farkas Z, et al. Iterative reconstruction algorithm for CT: can radiation dose be decreased while low-contrast detectability is preserved? Radiology 2013;269(2):511-518.

Schuberth JM, Christensen JC, Rialson JA. Metal-reinforced cement augmentation for complex talar subsidence in failed total ankle arthroplasty. J Foot Ankle Surg 2011;50(6):766-772.

Schwarz EM, Implant Wear Symposium 2007 Biologic Work Group. What potential biologic treatments are available for osteolysis? J Am Acad Orthop Surg 2008;16 Suppl 1:S72-75.

Singh G, Reichard T, Hameister R, Awiszus F, Schenk K, Feuerstein B, Roessner A, Lohmann C. Ballooning osteolysis in 71 failed total ankle arthroplasties. Is hydroxyapatite a risk factor? Acta Othop 2016;87(4):401-405.

Skytta ET, Koivu H, Eskelinen A, Ikavalko M, Paavolainen P, Remes V. Total ankle replacement: a population-based study of 515 cases from the Finnish Arthroplasty Register. Acta Orthop 2010;81(1):114-118.

Stradiotti P, Curti A, Castellazzi G, Zerbi A. Metal-related artifacts in instrumented spine. Techniques for reducing artifacts in CT and MRI: state of the art. Eur Spine J 2009;18 Suppl 1:102-108.

Stulberg BN, Della Valle AG, Implant Wear Symposium 2007 Clinical Work Group. What are the guidelines for the surgical and nonsurgical treatment of periprosthetic osteolysis? J Am Acad Orthop Surg 2008;16 Suppl 1:S20-25.

Tamaki Y, Sasaki K, Sasaki A, Takakubo Y, Hasegawa H, Ogino T, et al. Enhanced osteolytic potential of monocytes/macrophages derived from bone marrow after particle stimulation. J Biomed Mater Res B Appl Biomater 2008;84(1):191-204.

Tang H, Yang D, Guo S, Tang J, Liu J, Wang D, et al. Digital tomosynthesis with metal artifact reduction for assessing cementless hip arthroplasty: a diagnostic cohort study of 48 patients. Skeletal Radiol 2016;45(11):1523-1532.

Valderrabano V, Hintermann B, Dick W. Scandinavian total ankle replacement: a 3.7-year average followup of 65 patients. Clin Orthop Relat Res 2004;424:47-56.

Valderrabano V, Pagenstert G, Horisberger M, Knupp M, Hintermann B. Sports and recreation activity of ankle arthritis patients before and after total ankle replacement. Am J Sports Med 2006;34(6):993-999.

Valderrabano V, Pagenstert GI, Muller AM, Paul J, Henninger HB, Barg A. Mobile- and fixed-bearing total ankle prostheses: is there really a difference? Foot Ankle Clin 2012;17(4):565-585.

van Wijngaarden R, van der Plaat L, Nieuwe Weme RA, Doets HC, Westerga J, Haverkamp D. Etiopathogenesis of osteolytic cysts associated with total ankle arthroplasty, a histological study. Foot Ankle Surg 2015;21(2):132-136.

Vermes C, Roebuck KA, Chandrasekaran R, Dobai JG, Jacobs JJ, Glant TT. Particulate wear debris activates protein tyrosine kinases and nuclear factor kappaB, which down-regulates type I collagen synthesis in human osteoblasts. J Bone Miner Res 2000;15(9):1756-1765.

Vessely MB, Frick MA, Oakes D, Wenger DE, Berry DJ. Magnetic resonance imaging with metal suppression for evaluation of periprosthetic osteolysis after total knee arthroplasty. J Arthroplasty 2006;21(6):826-831.

Vickerstaff JA, Miles AW, Cunningham JL. A brief history of total ankle replacement and a review of the current status. Med Eng Phys 2007;29(10):1056-1064.

Viste A, Al Zahrani N, Brito N, Lienhart C, Fessy MH, Besse JL. Periprosthetic osteolysis after AES total ankle replacement: conventional radiography versus CT-scan. Foot Ankle Surg 2015;21(3):164-170.

Walde TA, Weiland DE, Leung SB, Kitamura N, Sychterz CJ, Engh CA,Jr, et al. Comparison of CT, MRI, and radiographs in assessing pelvic osteolysis: a cadaveric study. Clin Orthop Relat Res 2005;437:138-144.

Wang G, Yu H, De Man B. An outlook on x-ray CT research and development. Med Phys 2008;35(3):1051-1064.

Watzke O, Kalender WA. A pragmatic approach to metal artifact reduction in CT: merging of metal artifact reduced images. Eur Radiol 2004;14(5):849-856.

Wei X, Zhang X, Zuscik MJ, Drissi MH, Schwarz EM, O'Keefe RJ. Fibroblasts express RANKL and support osteoclastogenesis in a COX-2-dependent manner after stimulation with titanium particles. J Bone Miner Res 2005;20(7):1136-1148.

White AP, Vaccaro AR, Hall JA, Whang PG, Friel BC, McKee MD. Clinical applications of BMP-7/OP-1 in fractures, nonunions and spinal fusion. Int Orthop 2007;31(6):735-741.

Whittaker JP, Dharmarajan R, Toms AD. The management of bone loss in revision total knee replacement. J Bone Joint Surg Br 2008;90(8):981-987.

Willemink MJ, de Jong PA, Leiner T, de Heer LM, Nievelstein RA, Budde RP, et al. Iterative reconstruction techniques for computed tomography Part 1: technical principles. Eur Radiol 2013;23(6):1623-1631.

Willert HG, Semlitsch M. Reactions of the articular capsule to wear products of artificial joint prostheses. J Biomed Mater Res 1977;11(2):157-164.

Williams JR, Wegner NJ, Sangeorzan BJ, Brage ME. Intraoperative and perioperative complications during revision arthroplasty for salvage of a failed total ankle arthroplasty. Foot Ankle Int 2015;36(2):135-142.

Wood PL, Deakin S. Total ankle replacement. The results in 200 ankles. J Bone Joint Surg Br 2003;85(3):334-341.

Yoon HS, Lee J, Choi WJ, Lee JW. Periprosthetic osteolysis after total ankle arthroplasty. Foot Ankle Int 2014;35(1):14-21.

Zaidi R, Cro S, Gurusamy K, Siva N, Macgregor A, Henricson A, et al. The outcome of total ankle replacement: a systematic review and meta-analysis. Bone Joint J 2013;95-B(11):1500-1507.